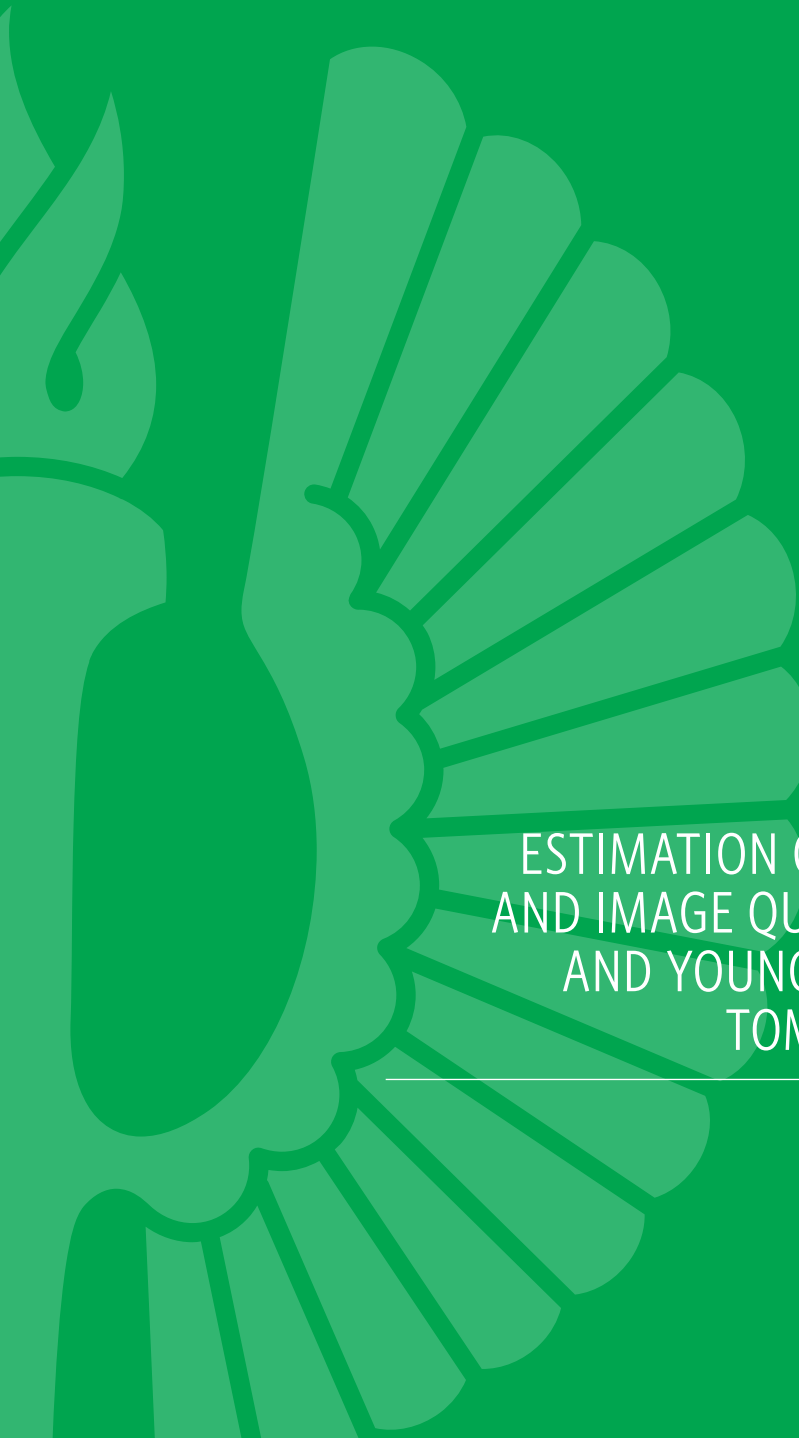




Turun yliopisto
University of Turku



ESTIMATION OF RADIATION DOSE
AND IMAGE QUALITY IN PEDIATRIC
AND YOUNG ADULT COMPUTED
TOMOGRAPHY STUDIES

Hannele Niiniviita



Turun yliopisto
University of Turku

ESTIMATION OF RADIATION DOSE AND IMAGE QUALITY IN PEDIATRIC AND YOUNG ADULT COMPUTED TOMOGRAPHY STUDIES

Hannele Niiniviita

University of Turku

Faculty of Medicine

Department of Radiology

Doctoral Programme in Clinical Research (DPCR)

Department of medical physics, Turku University Hospital and University of Turku

Medical Imaging Centre of Southwest Finland, Turku University Hospital

Supervised by

Professor Jarmo Kulmala
Department of Radiology
University of Turku, Finland

Adjunct professor Timo Kiljunen
Docrates Cancer Center
Helsinki, Finland

Professor Eeva Salminen
Radiation and Nuclear Safety Authority
Helsinki, Finland and
Department of Oncology
University of Turku, Finland

Reviewed by

Professor Hans Ringertz
Department of Radiology
Stanford University Medical Center
Stanford, CA, USA

Adjunct professor Paula Toroi
Section of Dosimetry and
Medical Radiation Physics
International Atomic Energy Agency
Vienna, Austria

Opponent

Professor Miika Nieminen
Department of Radiology
University of Oulu and Oulu University Hospital
Oulu, Finland

The originality of this thesis has been checked in accordance with the University of Turku quality assurance system using the Turnitin OriginalityCheck service.

ISBN 978-951-29-6941-8 (PRINT)

ISBN 978-951-29-6942-5 (PDF)

ISSN 0355-9483 (PRINT)

ISSN 2343-3213 (PDF)

Painosalama Oy - Turku, Finland 2017

*All our dreams can come true
– if we have the courage to pursue them.*
Walt Disney

ABSTRACT

Hannele Niiniviita

ESTIMATION OF RADIATION DOSE AND IMAGE QUALITY IN PEDIATRIC AND YOUNG ADULT COMPUTED TOMOGRAPHY STUDIES

University of Turku, Faculty of Medicine, Department of Radiology, Doctoral Programme in Clinical Research (DPCR), Department of medical physics, Turku University Hospital and University of Turku, Medical Imaging Centre of Southwest Finland, Turku University Hospital

Annales Universitatis Turkuensis

Painosalama Oy, Turku, Finland, 2017

Computed tomography (CT) is currently the most important contributor to medical radiation exposure, and pediatric and young adult CT studies raise special concern. A young age and high cumulative effective doses due to repeated CT during follow-up increase the risk of detrimental effects of radiation. Thus, the radiation dose, image quality, and the effects of parameter changes to these two need to be estimated to optimize CT examinations.

Thesis examines radiation doses as expressed by computed tomography dose index (CTDI), organ doses and effective doses among pediatric, adolescent and young adult patients. The influence of the CT scanner, patient size, and intravenous contrast agent were studied with regard to the radiation dose and image quality, and the effects of protocol parameter changes were studied to establish a more effective imaging protocol for the assessment of acute appendicitis. Radiation doses were evaluated by phantom measurements using dose monitoring software and dose calculation software. The image quality was evaluated by measuring the contrast to noise ratio and by visual assessment by radiologists.

A wide deviation of CT doses was found, despite homogenous cohorts and similar imaging indications. The deviation resulted from differences in the CT devices and non-optimized protocols. High effective doses cumulated during the follow-up of patients with testicular cancer. In the assessment of acute appendicitis, the radiation dose may be reduced, without decreasing image quality, by appropriate protocol adjustments. The large variations in radiation doses and the high cumulative effective doses emphasize the need for setting parameters carefully and for harmonized practices. There is also a need for improved dose monitoring, which may uncover non-optimized protocols.

Keywords: adolescent and young adults, computed tomography, image quality, pediatric, radiation dose

TIIVISTELMÄ

Hannele Niiniviita

SÄTEILYANNOKSEN JA KUVAN LAADUN ARVIOINTI LASTEN JA NUORTEN AIKUISTEN TIETOKONETOMOGRAFIA TUTKIMUKSISSA

Turun yliopisto, Lääketieteellinen tiedekunta, Radiologia, Turun kliininen tohtorihjelma (TKT), Lääketieteellinen fysiikka, Turun yliopistollinen keskussairaala ja Turun yliopisto, Varsinais-Suomen kuvantamiskeskus, Turun yliopistollinen keskussairaala

Annales Universitatis Turkuensis
Painosalama Oy, Turku Finland, 2017

Tietokonetomografia (TT) aiheuttaa nykyisin säteilyn lääketieteellisessä käytössä suurimman osan altistuksesta. Lasten ja nuorten TT-tutkimukset sekä seurannasta johtuvat toistuvat TT-tutkimukset ovat nousseet huolen aiheeksi, koska nuori ikä ja korkea kumulatiivinen efektiivinen annos ovat yhteydessä säteilyn haitallisiin vaikutuksiin. TT-tutkimusten optimoimiseksi säteilyannoksen suuruutta, kuvan laatua ja kuvausparametrien vaikutusta näihin pitää pystyä arvioimaan.

Tässä tutkimuksessa arvioitiin vastasyntyneen keuhkojen, lasten ja nuorten aikuisten pään ja kaularangan sekä kivessyövän seurannan aikana tehtyjen TT-tutkimusten säteilyannoksia. Käytettävän TT-laitteen, potilaan koon ja varjoaineen vaikutusta säteilyannokseen arvioitiin ja kuvausparametrien vaikutusta kuvan laatuun ja säteilyannokseen arvioitiin tehokkaamman protokollan löytämiseksi akuuttiin appendisiittiin. Säteilyannoksia arvioitiin fantomimittauksilla sekä annosseuranta- ja laskentaohjelmalla. Kuvan laatua arvioitiin mittamalla kontrasti-kohina suhdetta sekä visuaalisella arviolla.

Tutkimuksessa paljastui suurta vaihtelua säteilyannoksissa huolimatta yhtenäisestä kohortista ja indikaatiosta. Vaihtelu johtui erilaisista laitteista sekä epäoptimaalisista protokollista. Lisäksi havaittiin korkeita kumulatiivisia annoksia kivessyövän seurannassa. Akuutin appendisiitin tutkimisessa säteilyannosta voidaan alentaa kuvan laadun kärsimättä sopivalla parametrien muutoksella. Annosten suuri vaihtelu ja korkeat kumulatiiviset annokset osoittavat tarvetta protokollien säätämiseksi sekä yhtenäistämiseksi. Myös annoksien seurannalle on tarve, jotta mahdolliset epäoptimaaliset kuvausprotokollat saadaan havaittua ja korjattua.

Avainsanat: nuoret aikuiset, kuvan laatu, lapset, säteilyannos, tietokonetomografia

CONTENTS

ABSTRACT	4
TIIVISTELMÄ	5
CONTENTS	6
ABBREVIATIONS	8
LIST OF ORIGINAL PUBLICATIONS.....	10
1 INTRODUCTION.....	11
2 REVIEW OF LITERATURE.....	14
2.1 Radiation dose.....	14
2.1.1 Absorbed dose and organ dose.....	14
2.1.2 Equivalent dose and effective dose.....	14
2.2 Determination of radiation dose in CT.....	15
2.2.1 CTDI and DLP.....	16
2.2.2 Anthropomorphic phantoms and thermoluminescence dosimeters.....	17
2.2.3 Estimation of organ and effective doses.....	17
2.2.4 Dose monitoring.....	18
2.3 Image quality.....	19
2.3.1 Figure of merit.....	20
2.4 CT parameters in optimization.....	20
2.4.1 Tube voltage and x-ray energies.....	20
2.4.2 Contrast agents.....	22
2.4.3 Tube current modulation.....	23
2.4.4 Iterative reconstruction.....	25
3 AIMS OF THE STUDY.....	27
4 PATIENTS, MATERIALS AND METHODS.....	28
4.1 Phantoms.....	28
4.2 Patients.....	29
4.3 CT scanners and protocols.....	30
4.4 Dose measurements and estimation of effective dose.....	31
4.5 Image quality.....	33
4.6 Statistics.....	33
5 RESULTS.....	35
5.1 Radiation dose and image quality of CT studies of the chest of neonate (study I).....	35
5.2 Optimization of abdominal CT (study II).....	37

5.3	CTDI _{vol} and effective dose of CT studies of the head and cervical spine in the emergency department setting (study III)	40
5.4	Organ doses and cumulative effective doses from CT screening of testicular cancer (study IV)	44
5.5	Effect of CT scanner and IV contrast agent on radiation dose (study V).....	45
6	DISCUSSION	47
6.1	Effective dose.....	47
6.2	Radiation dose estimation in CT	48
6.2.1	CTDI _{vol} and DLP	48
6.2.2	Phantoms and TLDs.....	50
6.2.3	ImPact CTDosimetry	51
6.3	Study related risk	52
6.4	Optimization	53
7	CONCLUSIONS	57
	ACKNOWLEDGEMENTS	58
	REFERENCES	60
	ORIGINAL PUBLICATIONS	67

ABBREVIATIONS

AAPM	American Association of Physicist in Medicine
ALARA	As low as reasonably achievable
AP	Anteroposterior
AYA	Adolescent and young adult
BEIR	Biological Effects of Ionizing Radiation
BMI	Body mass index
CL	Confidence limit
CNR	Contrast to noise ratio
CT	Computed tomography
CTDI	Computed tomography dose index
CTDI _{vol}	Volume CTDI
CTDI _w	Weighted CTDI
<i>D</i>	Absorbed dose
DLP	Dose length product
DRL	Diagnostic reference level
DSB	Double-strand break
<i>E</i>	Effective dose
EFOMP	European Federation of Organizations for Medical Physics
ESR	European Society of Radiology
FBP	Filtered back projection
FOM	Figure of merit
<i>H</i>	Equivalent dose
HU	Hounsfield unit
IAEA	International Atomic Energy Agency
ICRP	International Commission of Radiologic Protection
ICRU	International Commission of Radiation Units and Measurements
IEC	International Electrotechnical Commission
IR	Iterative reconstruction
IV	Intravenous
ImPACT	Imaging Performance Assessment of CT Scanners
<i>K</i>	Kerma, kinetic energy released per unit mass
kVp	Peak kilovoltage
LAT	Lateral
<i>L</i>	Scan length
LNT	Linear no-threshold model
MBIR	Model-based iterative reconstruction
MOSFET	Metal-oxide-semiconductor field-effect transistor
MRI	Magnetic resonance imaging
NI	Noise input value

NCRP	National Council of Radiation Protection and Measurements
NRPB	National Radiological Protection Board
PACS	Picture Archiving and Communication System
PMMA	Polymethylmethacrylate
ROI	Region of interest
SD	Standard deviation
SSDE	Size-specific dose estimate
TCM	Tube current modulation
TLD	Thermoluminescence dosimeter
UNSCEAR	United Nations Scientific Committee on the Effects of Atomic Radiation
μ	Linear attenuation coefficient
ω_R	Radiation weighting factor
ω_T	Tissue weighting factor

LIST OF ORIGINAL PUBLICATIONS

This thesis is based on the following publications, which are referred to in the text by their roman numerals (I-V).

- I Niiniviita H, Kiljunen T, Kulmala J. Comparison of effective dose and image quality for newborn imaging on seven commonly used CT scanners. *Radiation Protection Dosimetry*, 2017;174(4):510-517
- II Niiniviita H, Salminen P, Grönroos J.M, Rinta-Kiikka I, Hurme S, Kiljunen T, Kulmala J, Teräs M, Sippola S, Virtanen J. Low dose CT protocol optimization in suspected acute appendicitis: the OPTICAP phantom study. *Radiation Protection Dosimetry*, 2017, doi:10.1093/rpd/ncx070
- III Niiniviita H, Kiljunen T, Huuskonen M, Teperi S, Kulmala J. Dose monitoring in pediatric and young adult head and cervical spine CT studies at two emergency duty departments. Submitted
- IV Salminen E, Niiniviita H, Kulmala J, Määttänen H, Järvinen H. Radiation dose estimation in computed tomography examinations using NRPB-SR250 software in a retrospective analysis of a patient population. *Radiation Protection Dosimetry*, 2012;152(4):328-333
- V Niiniviita H, Pölönen T, Kulmala J, Määttänen H, Järvinen H, Salminen E. Excess of radiation burden for young testicular cancer patients using automatic exposure control and contrast agent on whole-body CT-imaging. *Radiology and Oncology*, 2017;51(2)235-240

The original publications have been reprinted with the permission of the copyright holders.

1 INTRODUCTION

Computed tomography (CT) is the most important contributor to medical radiation exposure in the western countries. About 50 % of the collective effective dose in medical imaging originates from CT studies in Europe and USA, and in Finland the number is even slightly higher, 60 %. However, CT studies account for only 9 % –15 % of the total number of radiological procedures in these areas (EC, 2015; Mettler et al., 2008; Muikku et al., 2014; UNSCEAR, 2010). The CT examinations cause a significant amount of medical radiation exposure, because the radiation dose from a CT examination is higher than from conventional radiography, which constitutes the largest group of radiological studies. The radiation dose in CT is higher, because radiation is deposited from all entrance points around the patient, whereas in conventional radiography exposure is limited to one projection. The number of CT examinations has also increased rapidly since the introduction of CT in the early 1970's (UNSCEAR, 2010). The increase in the number of CT examinations has caused an increase in the population dose from medical radiation. In some countries, the biggest increase in CT studies has been in the pediatric population and in adult screening (Brenner and Hall, 2007), but in Finland the number of pediatric CT examinations has decreased (Suutari, 2016).

Although CT studies offer accurate diagnostic information, the use of ionizing radiation is problematic due to its detrimental effects, which are divided into two types by the International Committee of Radiation Protection (ICRP): deterministic effects and stochastic effects (ICRP, 2007). Deterministic effects, like skin erythema or epilation, only occur if the radiation dose is high enough to exceed a tissue-specific threshold value. Deterministic effects are rare in diagnostic imaging and usually occur only after abnormal events. The stochastic effects, like malignant tumors, are supposed to obey the linear no-threshold model (LNT), which assumes that low exposures increase the cancer risk in the same proportion as the exposure increases without any threshold (ICRP, 2007). The LNT model has been approved by the ICRP and the Biological Effects of Ionizing Radiation (BEIR) VII committee (BEIR, 2006; ICRP, 2007). The model is based on epidemiological data on atom bomb survivors of Hiroshima and Nagasaki, where the cancer incidence and mortality at higher effective doses (>100 mSv) have been extrapolated to lower effective doses (<100 mSv) (BEIR, 2006; ICRP, 2007).

Pediatric patients and young adults are more sensitive to radiation than older age groups. This follows from the cells of the developing organs and tissues dividing at a higher rate and from life expectancy allowing more time for harmful effects of radiation to appear (ICRP, 2013; Preston et al., 2007). Also, the average lifetime risk of cancer is higher in infants and young children compared with older children (ICRP, 1991).

Because of the possible detrimental effects of ionizing radiation, a considerable number of studies have raised great concern especially regarding pediatric patients. In the United

States alone, there were 85 million CT scans performed in 2011, 5–11 % of these on pediatric patients. It has been estimated that more than 4000 cancers could be induced by pediatric CTs of one year (Miglioretti et al., 2013). The exposure to CT studies increases the cancer incidence rate by 24 % in exposed patients compared to non-exposed patients aged 0 to 19 years (Mathews et al., 2013). Pearce et al. identified an association between pediatric head CT scanning and the increased risk of developing brain cancer and leukemia (Pearce et al., 2012). The possibility of deterministic effects of CT has also been raised, because brain CT in early childhood may affect cognitive abilities (Blomstrand et al., 2014; Hall et al., 2004).

In addition to pediatric patients and young adults, there is concern regarding patients who are imaged frequently during treatment and follow-up of illnesses (Brenner et al., 2003; Griffey and Sodickson, 2009). Frequent CT examinations increase the cumulative effective dose, but patients may still have a long life expectancy. High cumulative effective doses have been recorded among young patients with cancer, trauma or cystic fibrosis (O'Connell et al., 2012; Rohner et al., 2013; Sullivan et al., 2015).

There is no clear limit between safe and unsafe exposure – a corollary of the LNT model and the stochastic characteristics of radiation-induced adverse health effects. Thus, there is an obvious need for radiation protection, which is summarized into three principles by the National Council on Radiation Protection and Measurements (NCRP). These principles are justification, optimization and dose limitation (ICRP, 2013; ICRP, 2007; NCRP, 1993). The justification principle is fulfilled when the use of radiation has a net positive benefit. The optimization principle is fulfilled when the exposure is kept as low as reasonably achievable (ALARA). The optimization process includes reliable estimation of the dose, image quality assessment and knowledge of how the image parameters affect the radiation dose and image quality. The dose limitation principle states that the effective dose or equivalent dose shall not be exceeded set values in planned exposures. The principle of dose limitation is not used as such in medical exposure of patients, since the radiation dose is primarily determined by clinical needs. Instead diagnostic reference levels (DRLs) are used (EU, 2014; ICRP, 1996; ICRP, 2007). DRLs apply for routine conditions, and if DRLs are exceeded, a local review should be initiated to check whether optimization has been made and to assess if corrective actions should be taken. Unlike dose limits, DRLs do not induce constraints on radiation doses to individual patients (ICRP, 1996; ICRP, 2007).

The present work estimates the radiation dose as $CTDI_{vol}$, organ dose and effective dose and image quality of pediatric, adolescent and young adults (AYA) aged between 15 and 39 years. The effective dose and image quality of different scanners were estimated in neonates, the most vulnerable patient group with regard to radiation. The proportion of the radiation dose, out of the total radiation dose, caused by the localizer radiograph, not used in diagnostics, was studied as well. The radiation dose from head and cervical spine CT studies, common CT studies among children and AYA (Suutari, 2016), was estimated. The doses were compared to national DRL and the possibility to set local DRLs was studied.

Among AYA, acute appendicitis and follow-up of testicular cancer are common indications for CT (American Cancer Society, 2016; Sender and Zabokrtsky, 2015; Stark and Vassal, 2016). As the treatment of acute appendicitis is changing radically and patients are young, there is a need for a low dose protocol to differentiate complicated from uncomplicated appendicitis (Salminen et al., 2015). The parameters for abdominal CT were assessed to find an optimal protocol for assessment of acute appendicitis. The cumulative effective doses related to testicular cancer follow-up were estimated and the differences in radiation dose were assessed.

2 REVIEW OF LITERATURE

2.1 Radiation dose

In medical imaging, there are various dosimetric quantities used to assess the radiation dose to patients. These quantities are divided into basic quantities, application specific quantities and quantities related to the stochastic or deterministic effects of radiation. The term radiation dose refers to these quantities, where the basic quantities are kerma and absorbed dose, while the application specific quantities include descriptors like the computed tomography dose index and dose length product. Quantities related to harmful effects of radiation are equivalent dose and effective dose.

2.1.1 Absorbed dose and organ dose

The basic quantities are kerma (kinetic energy released per unit mass, K) and absorbed dose (D) (IAEA, 2007). Kerma is the sum of the initial kinetic energies (dE_{tr}) of all the charged particles liberated by uncharged particles in a mass of material (dm) as in equation 1.

$$K=dE_{tr}/dm \quad (1)$$

The absorbed dose is determined similarly with K . It is the mean energy (ϵ) imparted to matter per unit mass (dm) as seen in equation 2

$$D=d\epsilon/dm \quad (2)$$

The unit of K and D is joule per kilogram, but the special name, gray (Gy), is commonly used. The quantities have numerically equal values in the case of charged particle equilibrium. In x-ray imaging the equilibrium is achieved in low atomic number materials (IAEA, 2007; ICRU, 2005).

Organ dose (D_T) refers to the mean absorbed dose delivered to the organ or tissue. It is determined similarly as D in equation 2, where the mean energy (ϵ_T) is delivered to the specified organ or tissue with mass (m_T). The mean value of absorbed dose in an organ or tissue is related to biological effects and the protection quantities are based on organ doses (ICRP, 2007).

2.1.2 Equivalent dose and effective dose

Equivalent dose (H) and effective dose (E) are radiation protection quantities, which are used as a limit to ensure the occurrence of stochastic effects are kept acceptable and tissue reactions are avoided. The probability of stochastic events depends on the absorbed dose, the quality of radiation and the exposed organs. To consider the effects of these factors, the organ dose is weighted for radiation quality and radiation sensitivity of the organ. The

protection quantities as well as the weighting factors needed to calculate H and E were introduced by the International Commission of Radiologic Protection (ICRP). The ICRP 103 includes the latest update to these quantities and weighting factors (ICRP, 1977; ICRP, 1991; ICRP, 2007; ICRU, 2005).

H is defined as the sum of the mean dose absorbed by the tissue or organ on radiation quality R ($D_{T,R}$) multiplied with the radiation weighting factor (w_R). The value of w_R is 1 for x-ray radiation and H is calculated as shown in equation 3

$$H = \sum_R w_R D_{T,R} \quad (3)$$

E is the weighted sum of equivalent doses of organs of the body, defined in equation 4

$$E = \sum_T H_T w_T = \sum_T w_T \sum_R w_R D_{T,R} \quad (4)$$

where w_T is the weighting factor for a specific tissue or organ. Tissue weighting factors indicate the differences of probability of stochastic effects in different organs. They are derived from epidemiological studies of atomic bomb survivors and the risk assessment of inheritable diseases. The w_T s are presented in Table 1.

Table 1. Tissue weighting factors (w_T) for different organs and tissues according the ICRP 103 (ICRP, 2007).

Tissue/Organ	Weighting factor, w_T
Red bone marrow, breast, stomach, colon, lung, remainder*	0.12
Bladder, esophagus, liver, thyroid	0.04
Gonads	0.08
Bone surface, brain, skin, salivary glands	0.01

*Remainder organs are the adrenal glands, extrathoracic tissue, gall bladder, heart wall, kidneys, lymph nodes, muscles, oral mucosa, pancreas, prostate, small intestine, spleen, thymus and uterus/cervix.

The tissue weighting factors is an expression of the risk factors for both genders and all ages, and thus the effective dose is not used for estimating individual doses. However, the effective dose is practical and widely used for comparing radiation doses from different protocols or devices.

2.2 Determination of radiation dose in CT

Direct measurements of organ doses and E are limited by practical and ethical considerations, but organ doses and E are estimated by specific dose measurements using phantoms or by Monte Carlo calculations (ICRU, 2005). E can also be calculated from the dose display of a scanner with the aid of specific coefficients (Deak et al., 2010; Huda et al., 2008; Shrimpton, 2004).

2.2.1 CTDI and DLP

The computed tomography dose index (CTDI) is a standard metric used to express the absorbed dose; its value is related to scanner output (AAPM, 2008; ICRU, 2012). The International Atomic Energy Agency (IAEA) and International Commission on Radiation Units and Measurements (ICRU) recommend to use the CT air kerma index to express the radiation dose of CT examination, but in this thesis the more common term CTDI is used (IAEA, 2007; ICRU, 2005).

The CTDI is expressed as the integral of D along the z-axis for a single rotation as in equation 5

$$CTDI_{100} = \frac{1}{NT} \int_{-5cm}^{5cm} D(z) dz \quad (5)$$

where N is the number of simultaneously imaged sections in a single axial scan and T is the collimated slice thickness. The CTDI can be measured in air or in a cylindrical phantom by a 100 mm ionization chamber. The cylindrical phantom has a diameter of 16 cm for a head scan and 32 cm for a body scan, it is at least 14 cm long, and it is made of tissue-equivalent plastic, polymethylmethacrylate (PMMA). The length of the ionization chamber can be marked with a subscript after the CTDI and the subscript air is used for measurements made in air.

The exposure is not homogeneous in the body phantom; the measured CTDI is almost two times higher on the surface than in the center (ICRU, 2012). This heterogeneous distribution of exposure can be taken into account by using the weighted CTDI ($CTDI_w$) (AAPM, 2008; ICRU, 2005). $CTDI_w$ is calculated from the measurements made in the middle ($CTDI_c$) and in the periphery ($CTDI_p$) of the phantom as shown in equation 6

$$CTDI_w = \frac{2}{3} CTDI_p + \frac{1}{3} CTDI_c \quad (6)$$

The $CTDI_w$ does not consider of the gaps or overlaps of the beam during scanning, so the volume CTDI ($CTDI_{vol}$) is introduced to presents the absorbed dose over the x, y and z-directions (AAPM, 2008). It is calculated from $CTDI_w$ as in equation 7

$$CTDI_{vol} = \frac{NT}{b} CTDI_w = \frac{CTDI_w}{pitch} \quad (7)$$

where the pitch is the ratio between total collimation (NT) and table feed in one rotation (b). The $CTDI_{vol}$ expresses the mean absorbed dose of a helical scan a in dosimetric phantom, and the total amount of radiation is estimated by the dose length product (DLP), where the $CTDI_{vol}$ is multiplied with the total scan length (L) as in equation 8 (AAPM, 2008).

$$DLP = CTDI_{vol} \times L \quad (8)$$

The $CTDI_{vol}$ and DLP are widely used for expressing the radiation dose from a CT study. These quantities are useful for comparing different scanners and different protocols, as they

are related to scanner output and scan length. Further, the effective dose can be roughly estimated from DLP by using conversion factors fixed to the anatomic region and age of the patient. The coefficients are derived from the relationship between the calculated effective dose and DLP (Huda et al., 2011; Shrimpton et al., 2005).

2.2.2 Anthropomorphic phantoms and thermoluminescence dosimeters

Since organ dose measurements cannot – for practical purposes – be made *in vivo*, specific phantoms used together with dosimeters are a good substitute for estimating organ doses. The anthropomorphic phantoms are made from tissue equivalent plastic. They come in different sizes and imitate absorption and scattering as they occur in patients. The plastic compositions typically simulate bone, soft and lung tissue and the sizes and compositions of the phantoms are based on reports like ICRP 23 and ICRU 48 (ICRP, 1979; ICRU, 1992). The plastic phantoms may consist of slabs with drilled holes for dosimeter placement. Measurement with dosimeters placed inside phantoms express only the absorbed dose of individual points, but organ doses can be estimated from these point doses.

The anthropomorphic phantoms are often used with thermoluminescence dosimeters (TLD). TLDs have many advantages for when measuring absorbed dose: small size; very sensitive to radiation; and tissue equivalence, which is essential for the determination of biologically meaningful radiation doses since scattered radiation contributes significantly to the radiation dose. These features make them appropriate for dosimetrics (Kron, 1999).

The use of TLDs to determine absorbed doses is based on ability of the material to absorb and store radiation energy. Radiation excites electrons of the TLD material to higher metastable energy states. When heated, sufficient thermal energy is given to the electrons and they return to the ground state simultaneously emitting visible light. The amount of light is presented as a glow curve and it is dependent of heating temperature, TLD material and absorbed dose. The light is collected with photomultiplier tube. The intensity of the light is proportional to the absorbed dose. The area under the glow curve corresponds to the absorbed dose once calibration has been made. Calibration is made by exposing the TLDs to a known reference radiation source, after which the intensity of the emitted light can be linked to the absorbed dose (ICRU, 2005).

2.2.3 Estimation of organ and effective doses

In addition to phantom measurements, organ doses can be estimated with Monte Carlo simulations of photon paths and interactions. The information is then used to evaluate the dose absorbed by a material. These simulations need a model of patient anatomy and a radiation source. Computational human models are used for patient anatomy, and the models are either mathematical or voxel phantoms (ICRP, 2009; ICRU, 2005). Phantom models of different sizes to suit different ages and both genders are being developed (Norris et al., 2014; Segars et al., 2013, 2008).

In this thesis, a spreadsheet of ImPACT CTDosimetry was used, which is designed to calculate the organ doses and effective doses generated in CT examinations (Impactscan.org/ctdosimetry.htm). The spreadsheet utilizes so called data set which consists of Monte Carlo calculations made by the National Radiological Protection Board (NRPB). The spreadsheet includes 23 data sets which model the exposure conditions of 27 CT scanners. One data set consists of 208 slices, where one slice corresponds to the absorption of one rotation over the phantom. The slices are 5 mm thick and cover the hermaphrodite phantom from the top of the head to the lower limbs. Monte Carlo simulation is used to model the absorption and scattering within these slices and the absorbed doses are normalized to CTDI in the air and tube current-rotation time product for later calculations (Jones and Shrimpton, 1993).

The same data sets can also be used with other scanners than the original 27 ones used for modelling. A data set for a specific scanner is selected by measuring CTDI in the air and in the central and peripheral positions in head and body phantoms and then by determining the so-called ImPACT factor from these measurements. The determined ImPACT factor is compared to the ImPACT factors of the original scanners and the same data set is used with similar ImPACT factors (Shrimpton et al., 2005). The ImPACT group has already added scanners to the spreadsheet and the current version (1.0.4) of ImPACT CTDosimetry includes 75 scanners.

2.2.4 Dose monitoring

CT scanners report $CTDI_{vol}$ and DLP after the examination as required by the International Electrotechnical Commission (IEC) standard (EC, 2012; IEC, 2009). Since many variables, e.g., protocol parameters and patient anatomy, affect the $CTDI_{vol}$ and DLP values, it is essential to continuously monitor these doses to ensure that the radiation dose is kept at an acceptable level in the examinations. Systematic dose monitoring is an essential part of quality assurance: scanner-reported doses are compared to DRLs in an effort to recognize excessive radiation doses. Fulfilment of the ALARA-principle can thus be evaluated by assessing and monitoring the dose display values (Boos et al., 2016; EC, 2012; Miller et al., 2015).

Manual registration of dose metrics is time-consuming and prone to errors. Recently, vendors have introduced proprietary software tools for automatic collection and analyzing of dose data. The dose monitoring software collects the exposure information from PACS (picture archiving and communication system) or, alternatively, the CT scanners transmit the data directly to the software. These software tools enable the collection and analysis of large amounts of data and they offer reports which allow easier distinguishing of deviations and optimization (Boos et al., 2016; Higashigaito et al., 2016). The dose monitoring software tools can be used for optimization by comparing the dose display values and image parameters among different scanners, but they are also valuable for comparing dose display values with DRLs and setting local DRLs. The DRLs are introduced in $CTDI_{vol}$ and DLP values

for CT studies. The DRLs are usually set at the 75th percentile of radiation doses and a radiological protection authority sets DRLs on the national level (EC, 1999; ICRP, 2007). The higher the number of patients, the better the reliability when a new DRL is set, and the same holds true for the reliability when comparing radiation doses to DRLs. The DRL should not be applied for an individual, but only compared to the average CT study dose (EC, 1999).

2.3 Image quality

The image quality of CT studies is usually described in terms of image noise, image contrast, spatial resolution and artifacts. These factors determine the visibility of structures and details, and the clinical indication determines the required level of image quality. Contrast and noise are the fundamental factors in image quality: high noise or low contrast makes the objects invisible regardless of resolution.

Contrast means the overall difference in the greyscale of the image. Contrast is defined as the ratio of the signal difference to the signal of background and can be calculated as shown in equation 9

$$C = \frac{HU_a - HU_b}{HU_b} \quad (9)$$

where the HU_a and HU_b are the measured Hounsfield units of the object of interest and the background of the object, respectively (see section 2.4.1).

Noise is an important determinant of image quality, because excess noise can reduce image resolution and impair the detection of low-contrast objects from background. Noise is defined as the standard deviation (SD) of the HUs in the image of uniform substance (ICRU, 2012). Noise can be derived from the x-ray detection system itself as electronic noise, but with current scanners quantum noise is more probable. Quantum noise is associated with the number of photons and the number of photons is, in turn, associated with radiation dose. The relationship between quantum noise and radiation dose is well known: noise is inversely proportional to the square root of the radiation dose and the radiation dose is directly proportional to the number of x-ray quanta (Bushberg et al., 2012). Thus, tube current adjustment becomes an attractive way to optimize, since the relationship between tube current and image quality is straightforward, if other parameters are kept constant. Indeed, tube current adjustment is one of the most common tools in controlling radiation dose.

Contrast and noise can be compounded as one variable, because the visibility of low-contrast objects is dependent on contrast and on noise. In some cases, the contrast to noise ratio (CNR) can be used as a measure of image quality.

2.3.1 Figure of merit

The evaluation of image quality is essential when optimizing protocols. Image quality must be of a certain standard, so that the CT images are diagnostic, but the radiation dose must be kept low according to ALARA principle. Figure of merit (FOM) is a quantity, which can be used to compare different protocols, since differences in beam quality and tube current prevent direct comparisons of image quality between different protocols. The purpose of FOM is to make image quality independent of radiation dose, when it is feasible to compare different scanners or different protocols (Samei et al., 2005; Verdun et al., 2015).

In general, amount of radiation which is required to achieve a certain level of image quality (Verdun et al., 2015). There is no a single FOM in use, which would consider all image parameters, but one of the straightforward FOM is to normalize the CNR to the radiation dose. This version of FOM has been used especially for comparing protocols with different tube voltages; it is calculated as shown in equation 10

$$FOM = \frac{((HU_a - HU_b)/SD_b)^2}{dose} = \frac{CNR^2}{dose} \quad (10)$$

where HU_a and HU_b are the HUs of the object and the background respectively, and the SD_b is the noise of the background. CTDI, effective dose or some other suitable dose parameter can be used as a dose for calculating the FOM (Kim et al., 2017; Marin et al., 2010; Verdun et al., 2015; Wichmann et al., 2017).

The FOM enables the assessment of CNR independently of the tube current and radiation dose. However, as it is determined for a specific scan mode (helical or axial) and for a specific diagnostic task, it should not be used for comparing different scanned areas or diagnostic tasks, e.g., when comparing head and abdomen imaging (Kalender, 2011).

2.4 CT parameters in optimization

Image quality and radiation dose are related to the patient and the clinical task, but so are a number of imaging parameters. Thus, radiation dose reduction without compromising image quality is not straightforward, and for protocol optimization it is essential to understand and evaluate the effects of the different parameters on image outcome. The typical adjustable parameters are tube voltage, tube current and level amount of iterative reconstructions (Goo, 2012; Mayo-Smith et al., 2014).

2.4.1 Tube voltage and x-ray energies

Tube voltage refers to the voltage applied across the x-ray tube. The tube voltage is expressed as the peak kilovoltage (kVp) which is the maximum voltage across the tube. In the x-ray tube, electric voltage accelerates electrons from the cathode to the anode and the kinetic energy of these electrons is converted to x-ray photons and heat, as the electrons

lose their kinetic energy at the anode. The unit electronvolt (eV) is often used to express the kinetic energy of electrons and the energy of photons.

The image contrast is related to the x-ray attenuation in different tissues and organs. The amount of attenuation is dependent of photon energy as well as the features of the attenuating material. At diagnostic x-ray energy levels, photons are attenuated by absorption, which provides a photoelectric effect, and by Compton scattering. The probability of different interactions as a function of energy in soft tissue is presented in Figure 1 (Bushberg et al., 2012).

In the photoelectric effect, all of the energy of the x-ray photon is used to eject an electron from an atom and to the kinetic energy of electron. Thus, the absorbed photons are not detected by the detector (Bushberg et al., 2012). The probability of absorption depends on the energy of the photons (E_p) and on the density (ρ), atomic number (Z) and atomic mass (A) of the attenuating material. Attenuation is best expressed in the formula for the linear absorption coefficient for the photoelectric effect (μ_p):

$$\mu_p = \frac{\rho Z}{AE_p^3} \quad (11)$$

The image contrast decreases at higher energies, because the absorption is inversely related to energy cubed, as can be seen in equation 11 (Bushberg et al., 2012; Lusic and Grinsta, 2012).

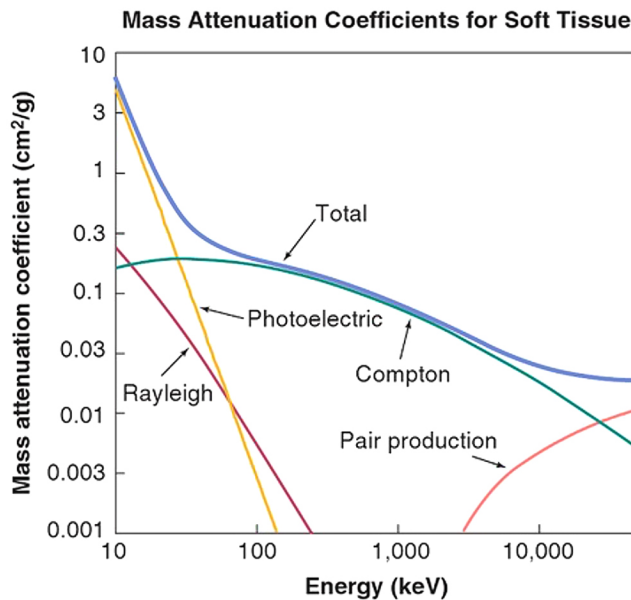


Figure 1. X-ray interactions with matter as a function of energy. Reprinted with permission from the copyright holder (Wolters Kluwer) (Bushberg et al., 2012).

With higher energies (above 30 keV) the photons are more probably attenuated by Compton scattering. The attenuation resulting from Compton scattering is denoted with μ_c . Scattering is the predominant interaction in the diagnostic energy range, and, in addition to energy, the probability of Compton scattering depends on the electron density of the attenuating material. Scattering impairs image quality, because it alters the direction of the photons which will be detected by a wrong detector. Thus, the scattered photons introduce contrast-reducing background or noise to the image (Martin, 2007a). In addition to contrast, tube voltage is related to x-ray production. The tube produces photons more efficiently at higher tube voltages, but the relationship is non-linear, as photon production is approximately proportional to tube voltage squared. The number of photons is related to noise and radiation dose (Bushberg et al., 2012).

The differences of attenuation in different organs and tissues are presented by CT numbers instead of the linear attenuation coefficient μ . The linear attenuation coefficient is the sum of the individual linear attenuation coefficients for each interaction (μ_p and μ_c). The CT numbers, called Hounsfield units (HU), express the linear attenuation of material in relation to the linear attenuation of water, as shown in equation 12

$$HU = \frac{\mu - \mu_w}{\mu_w} \times 1000 \quad (12)$$

where μ_w is the linear attenuation coefficient of water (Lusic and Grinstaff, 2012).

2.4.2 Contrast agents

Optimal tube voltage is typically determined by patient size and the type of CT examination, but the selection of the optimal tube voltage is not straightforward, since tube voltage affects contrast and noise (Kalra et al., 2004). Patient size affects the attenuation of photons and for small patients appropriate image quality can be obtained with lower tube voltages. For large adults, the use of low tube voltage is not recommended, because low tube voltage can produce high noise and introduce photon starvation artifacts in the image (Karmazyn et al., 2013; Yu et al., 2011). The contrast can be increased in CT studies with the use of intravenous (IV) contrast agents, which are iodine-based saline solutions. Contrast agents enhance vessels and organs due to the fact that hypervascular and hypovascular structures are seen better in images (Yu et al., 2011). Lower tube voltages are possible when IV contrast is used and higher contrast can be achieved. At lower energies the mean photon energy approaches the K-edge of iodine (33 keV) and the probability of a photoelectric effect increases abruptly as can be seen in Figure 2 (Goo, 2012; Huda et al., 2000).

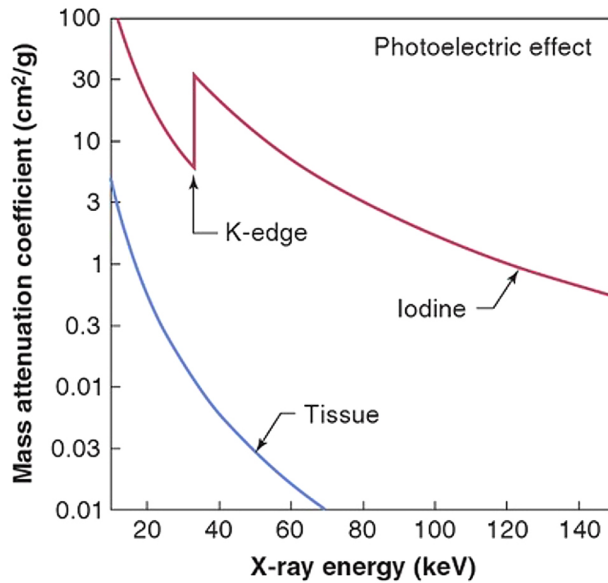


Figure 2. Total attenuation of x-rays in different materials as a function of energy. The absorption in iodine increases abruptly when photon energy exceeds 33 keV. Reprinted with permission from the copyright holder (Wolters Kluwer) (Bushberg et al., 2012).

2.4.3 Tube current modulation

The use of a constant tube current is problematic in CT imaging due to variations in patient attenuation by anatomic regions and by anteroposterior (AP) and lateral (LAT) directions. To achieve a more stable radiation dose at detector level and thus more stable image quality independent of the region or projection angle, tube current modulation (TCM) was developed. To achieve a constant noise level throughout the images, TCM sets the tube current level by patient size and TCM modulates the tube current in real time in the axial plane (the x-/y- directions) as well as along the patient (the z-direction). The modulation considers the size and shape of the patient and the attenuation of the scanned parts (McCollough et al., 2009).

When TCM modulates the current angularly (x- and y- directions), it is called α -modulation. As the noise patterns are oriented in the direction of the highest attenuation (LAT), the tube current can be reduced for lower attenuation directions (AP/PA) without deleterious effects on image quality. This reduces the total current, as the reduction in the radiation dose is mostly due to α -modulation. In fact, the central organ doses decrease more than the tube current-rotation time-product would predict. Since radiation attenuates less in the AP-direction than in the LAT-direction, the absorbed dose to the organs is caused mostly by exposure in the AP-direction. Thus, the central organs undergo stronger absorbed dose reduction, when the current is reduced in the AP-direction. The modification of the angular TCM is dependent on the shape of the region: heterogeneous regions need stronger modulation than uniform regions (Kalender et al., 2008).

Longitudinal modulation modulates the tube current in the z-direction. It compensates for the varying attenuation along the patient so that image quality is sufficient for the whole region of the scan. The objective of the z-axis TCM is to keep image quality on a preset level along the z-axis, where smaller parts are scanned with lower tube currents. The angular and longitudinal TCM can be operated simultaneously and when used properly TCM may decrease the radiation doses of CT studies by 20–40 % (Kalender et al., 2008; McCollough et al., 2009). The function of TCM is presented in Figure 3.

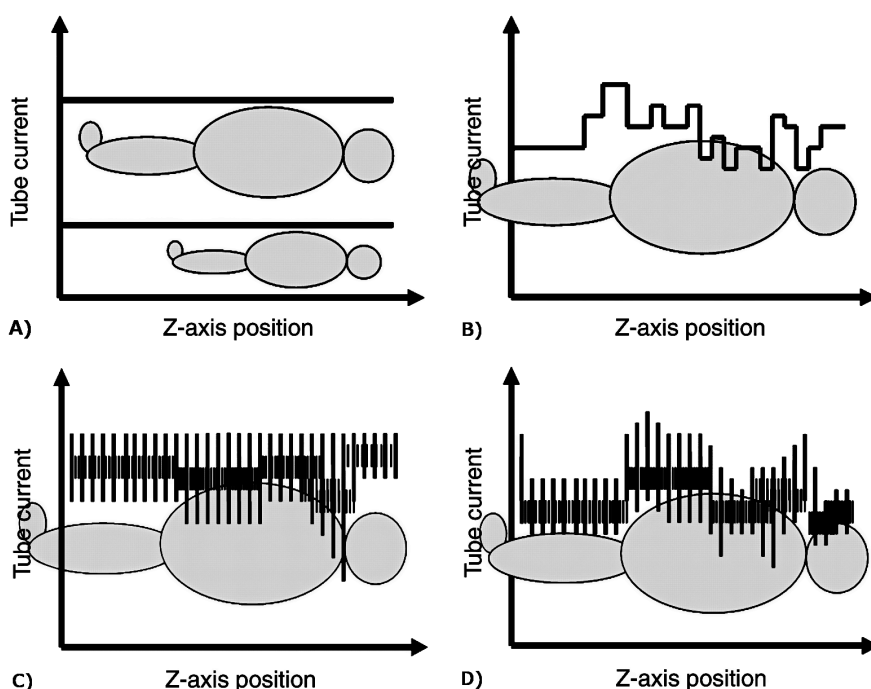


Figure 3. Illustration of types of tube current modulation (TCM). The level of tube current depends on patient size (A), the tube current modulates according to patient attenuation along the z-axis (B), the tube current modulates according to patient attenuation in the x/y-plane (C), the tube current modulates according to the combined effects (D). Reprinted with permission from the copyright holder (RSNA) (Lee et al., 2008).

The scanners determine the attenuation of the patient by using one or two localizer radiographs, and based on these attenuation values, the amount of current is determined together with a noise input (NI) value. The NI values are related to the noise level of the final image and they depend on the scanner and image parameters. The NI values are set by the operator and the optimal values depend on the clinical indication as well as on patient size: more noise can be tolerated with larger patients (Soderberg and Gunnarsson, 2010). The proper function of the TCM assumes that the patient is positioned in the isocenter of the gantry, when the attenuation data is correct. In addition, the scanners have a bowtie

filter, which attenuates the radiation more on the periphery than in the middle, thus compensating for patient absorption before the detector. If the patient is miscentered the TCM and bowtie filter do not work optimally, and radiation dose and image noise are affected (Kaasalainen et al., 2013; Matsubara et al., 2009).

2.4.4 Iterative reconstruction

Historically, the first clinical CT studies used iterative reconstruction (IR) for image formation, but IR was superseded by filtered back projection (FBP) which has faster image calculation. Computational capacity has grown exponentially during the past decades, and this has rekindled the interest in IR which has become a realistic alternative for image reconstruction again (Beister et al., 2012). IR is an interesting choice for optimization, because, unlike FBP, it enables noise reduction by calculating the images multiple times. Furthermore, noise reduction allows the use of CT techniques with lower tube current or tube voltage without compromising image quality. Algorithms also improve resolution by maintaining edges and removing artifacts in the image (Padole et al., 2015).

The first step in IR is to make an initial estimate of the object. The estimate can be an empty image or prior information, *e.g.*, an FBP image or a volume of a similar object. The more accurate the initial estimate is, the faster the IR process becomes. The image estimate is forward projected, so that it can be compared with the measured data. Depending on the IR algorithm, the forward projection can include a model of scanner-specific geometrics, x-ray properties or the photon distribution. The differences in forward projected data and measured projections are used to update the initial estimate, which is forward projected after corrections and the IR cycle starts over. The IR cycle is terminated when a fixed number of iterations has been made, predefined image quality criteria have been reached or the update for the image estimate is considered to be small enough (Beister et al., 2012; ICRU, 2012; Mayo-Smith et al., 2014). The principle of IR is presented in Figure 4.

In this thesis, hybrid IR methods are used, where FBP and IR images are blended together. The impression of the image is more FBP-like, when the images are blended. Still, radiologists need time to adapt to the new images, because noise patterns and artifacts appear differently (Beister et al., 2012). Another disadvantage of IRs is that they are vendor specific, which hampers comparisons, and undesirable artifacts such as texture or blotchy appearances with high strengths of IR have been reported (Kim et al., 2014). Long reconstruction times are still a problem, especially with novel model-based iterative reconstructions (MBIR). MBIRs are fully iterative techniques, which attempt to model the acquisition process as accurately as possible (Beister et al., 2012). The use of IR has proved to result in a significantly lower (23–66 %) radiation doses to patients undergoing CT studies compared to FBP (Sagara et al., 2010; Thomas et al., 2015), and MBIR has lowered the radiation dose further.

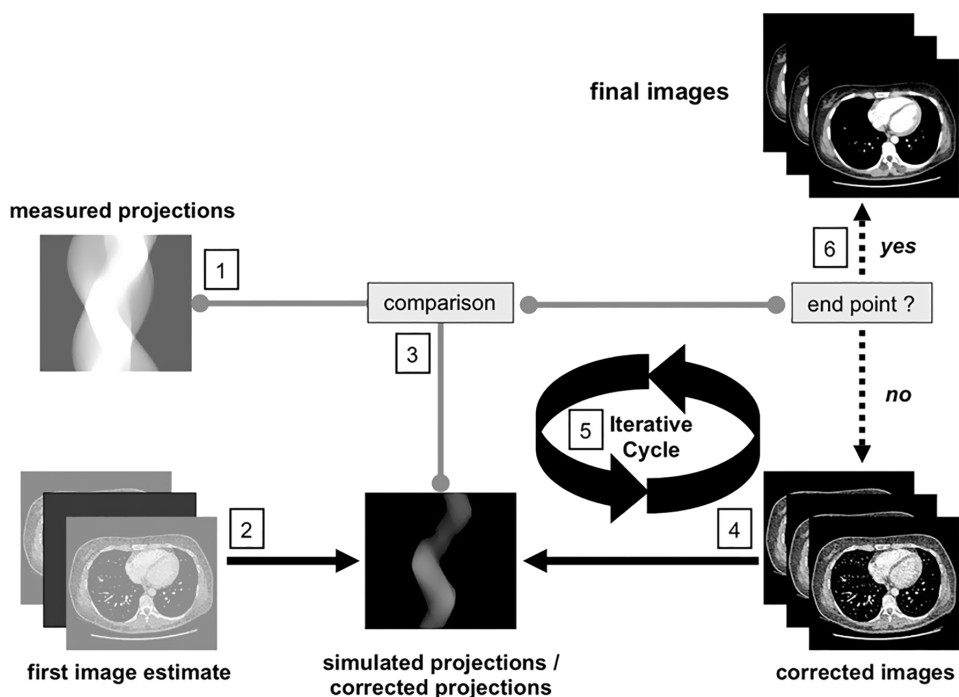


Figure 4. Steps of iterative reconstruction (IR). First image estimates (2) are produced from measured projections (1) and the simulated projections made from image estimations are compared with measured projections (3). If endpoint criteria are not fulfilled, the algorithm makes corrections to the image (4) and cycle is repeated (5) until an endpoint is reached. Reprinted with permission from the copyright holder (RSNA) (Geyer et al., 2015).

3 AIMS OF THE STUDY

The aims of this study were to investigate image quality and radiation dose when CT scanners with different features and parameters are used. The specific aims were:

- I. to compare organ doses and effective doses to neonates undergoing chest CT with different CT scanners estimated by three methods and to compare the effective dose of the localizer radiographs in this setting.
- II. to study the effects of tube voltage, IR and NI on image quality and $CTDI_{vol}$ and to study the CNR and FOM at different protocols to find the most effective protocol for CT-examinations indicated by a suspicion of acute appendicitis.
- III. to study the influence of the CT scanner and age on $CTDI_{vol}$ and to assess the possibility to set local DRL values for pediatric and young adult head and cervical spine CT in the emergency department.
- IV. to study the cumulative effective doses to patients who have been scanned repeatedly for testicular cancer follow-up and to investigate the organ doses and effective doses from different CT scanners used during follow-up.
- V. to investigate the effect of different CT scanners and IV contrast agents on the effective dose in whole body CT studies.

4 PATIENTS, MATERIALS AND METHODS

4.1 Phantoms

In studies I and II, the doses from different CT scanners and protocols were assessed with the use of anthropomorphic phantoms, which were made from tissue equivalent plastic. In study I, an ATOM pediatric newborn phantom (model 703-D, CIRC, Norfolk, Virginia, USA) was used. It corresponds to the average size of a newborn, 3.5 kg and 50 cm, and consists of 2.5 cm thick slabs with drilled holes for TLDs of different organs. The phantom included tissue equivalent lungs and bones. The phantom is seen in Figure 5 A.

In study II, a torso phantom was used (Scandnordax, Vallentuna, Sweden). It consisted of ribs, the spine and a piece foam, with 15 test tubes fastened to it. The foam was inserted in the abdominal part of the phantom. Otherwise the phantom was hollow and was filled with water. To achieve more attenuation, the phantom also had an additional plastic piece on the ventral side, which was 5 cm thick at the thickest point. The phantom including the foam and test tubes are shown in Figure 5 B. The inner diameter of the test tubes was 10 mm, which is approximately of the same size as an infected appendix. Fourteen of the test tubes were filled with various concentrations of iodine solution and one with an appendicolith to estimate the contrast in relation to water and the other tubes. The test tube with the appendicolith was filled with water.

The different iodine concentrations were created by serial dilution of Omnipaque 350 mg/ml (GE Healthcare, Wisconsin, USA) in saline. The starting point of the serial dilution was 1:40, which is the standard ratio when IV contrast is used, and the serial dilution was made at a ratio of 3:4. By using serial dilution, it was possible to achieve similar HU values as are produced clinically by the contrast material and the different tissues. The actual concentrations were 8.75, 6.56, 4.92, 3.69, 2.77, 2.08, 1.55, 1.17, 0.88, 0.66, 0.49 and 0.37 mg/ml. One tube was filled with saline only and one tube with contrast at a concentration of 2.57 mg/ml, which was assumed to be the visibility threshold based on preliminary tests.

In studies I, IV and V the ImPACT (Imaging Performance Assessment of CT Scanners) CTDosimetry (version 1.0.4) was used. This is a calculator tool in the form of a spreadsheet for calculating patient organ doses and effective doses from CT examinations. It uses Monte Carlo simulated data sets calculated by NRPB, which provide normalized organ-specific doses in a mathematical phantom (Jones and Shrimpton, 1993). The phantom is an adult sized hermaphrodite and consists of a body and a head.

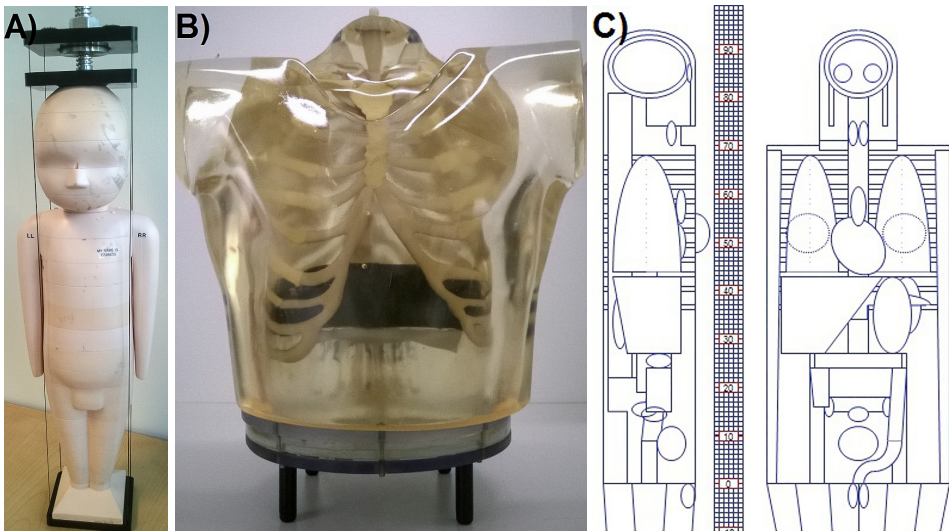


Figure 5. Phantoms. An ATOM newborn phantom (A) was used in study I, abdomen-thorax phantom (B) in study II and a mathematical ImPACT CTDosimetry phantom (C) in studies I, IV and V. The test tubes are located below the foam in the abdomen-thorax phantom (B). The CTDosimetry phantom is downloadable together with an excel spreadsheet at www.impactscan.org/ctdosimetry.htm.

When approximating the pediatric dose from this phantom, a factor of 2.2 was used for effective dose as proposed by the spreadsheet, the scan region was fitted to the CTDosimetry phantom and the actual length was ignored in the calculations (Khursheed et al., 2002). The phantom is shown in Figure 5 C.

4.2 Patients

In study III, dose monitoring software (DoseWatch, GE, Wisconsin, USA) was used to collect the CT study related data. Patients under the age of 21 years attending the Emergency Department who required a routine head, trauma head or trauma cervical spine CT study between 1 June 2014 and 1 June 2016 were included. An Aquilion One (Toshiba, Otawara, Japan) or a Definition Flash Dual (Siemens, Erlangen, Germany) CT device was used for imaging.

There were 1526 studies: 319 routine studies of the head, 615 trauma head and 592 trauma cervical spine. The patients were categorized into four age groups for $CTDI_{vol}$ assessment (0–5, 6–10, 11–15 and 16–20 years).

In study IV, there were 122 testicular cancer patients, who were scanned during cancer follow-up at the Turku University Hospital between the years 1994 and 2011. The details of radiological examinations (image parameters, scanning length and scanning area) were retrieved from the picture archive system (PACS) (Carestream, New York, USA) of the Turku University Hospital for 111 (91%) of these patients.

The data for study V was extracted from the data of study IV. The inclusion criteria were age under 40 years, CT study of the whole body and examined with either the LightSpeed 16 (General Electric, Milwaukee, USA) or the Plus 4 (Siemens, Erlangen, Germany). The inclusion criteria were fulfilled by 65 patients. The effect of patient size on the radiation dose was roughly estimated by dividing the patients into two groups by their waist circumference: above and below 100 cm. The waist circumference was measured from the PACS images at the midpoint between the lowest rib and the iliac crest. The waist circumference was used because it was a more reliable predictor of patient size than body mass index (BMI) in this setting, since data on height and weight were often missing.

For study III, there was no need for approval by local ethical committee according to the Finish legislation (Ministry of Social Affairs and Health, 2016). For studies IV and V, approval by the Ethics Committee of Hospital District of Southwest Finland was obtained (ETMK 109/2011, 304 §).

4.3 CT scanners and protocols

In study I, the newborn phantom was scanned once with seven different CT scanners and five times with one scanner to estimate repeatability. The scan region was 100 mm long and covered the thorax region. The used scanners were LightSpeed 16 and Optima 660 (General Electric, Milwaukee, USA), Somatom Sensation 64 and Definition Flash Dual (Siemens, Erlangen, Germany), Aquilion 32, Aquilion Prime and Aquilion One (Toshiba Medical Systems, Otawara, Japan). In study I, all of the CTs used their own specific protocol on pediatric imaging. The Sensation 64 is routinely used for pediatric studies, but all other CTs used non-optimized protocols.

In study II, the abdomen-thorax phantom was scanned with the Aquilion Prime scanner with 66 different protocols. The tube voltage and IR together formed six different combinations, as the tube voltage was either 80 kVp, 100 kVp or 120 kVp and the IR was set on a standard or strong level, where the IR level determines the number of iterations and the percent of blending between filtered back projected and iteration reconstructed images. The six protocols were defined as: A=80 kVp standard IR, B=80 kVp strong IR, C=100 kVp standard IR, D=100 kVp strong IR, E=120 kVp standard IR and F=120 kVp strong IR. The protocols were used with eleven different noise input values (NI). The NI started from 10.5 and increased with 1 NI until reaching a value of 20.5, which covers the NI range of abdominal imaging in our departments for the Aquilion Prime or One scanners. As a result, 66 different protocols were studied. All other parameters were kept constant: rotation time 0.5 s, pitch 0.813, detector configuration 0.5 x 80 mm, Kernel FC07 and scan length 132 mm in the abdominal region.

In study III, data was collected from two emergency departments that used the Definition Flash Dual and Aquilion One scanners. Both devices were used in study I, as well. The

collected data was exported for analysis to a Microsoft Excel spreadsheet (version: 14.0.7172.5000, Microsoft Office, Washington, USA).

In study IV, 15 different scanners from four vendors had been used to make 780 studies made of the head, thorax, abdomen and whole body of 111 patients with testicular cancer. The details of 665 CT studies were retrieved (85%).

From study IV two of the scanners were selected for further review for study V. The scanners were the LightSpeed 16 (General Electric, Milwaukee, USA) and the Plus 4 (Siemens, Erlangen, Germany). Study V only consisted of whole body scans, which amounted to 279 examinations for 65 testicular cancer patients.

4.4 Dose measurements and estimation of effective dose

The thermoluminescence dosimeters (TLD), dose display of the scanner and the ImPACT CTdosimetry tool were used to estimate the effective dose and organ doses. In study I, all of them were used, in study II and III, only the dose display of the scanner was used, and in studies IV and V, only the ImPACT CTdosimetry tool was used.

The TLDs in study I were calibrated before use with a reference irradiator by RADOS OY (RADOS Technology Oy, Turku, Finland) by using ^{137}Cs and 1.0 mGy absorbed dose. The material of the TLDs (TLD Poland, Krakow, Poland) was MCP-N (LiF: Mg, Cu, P), which has a detection threshold of 50 nGy. The TLDs were annealed before scanning and the annealing and read out were performed with a specific TLD reader. There were 16 TLDs, which were inserted in the pediatric phantom. They were placed inside thyroid, lungs (four TLDs), rib, sternum, spine, liver (two TLDs), one in both kidneys, two TLDs in the region of the bowels, hip and ovary. The effective dose was roughly estimated by substituting the results of TLD measurements ($D_{T,R}$) and coefficients of ICRP 103 (w_T) in equation 4 (ICRP, 2007). The dose of the nearest TLD was used for the evaluation of those organs, whose dose was not directly measured by a TLD, and the dose of the area outside the scan area was assumed to be 10 % of the measured dose. This was done to minimize the effect of localizer radiographs, since localizer radiographs extended over the CT scan area. The stomach and liver were not scanned fully, because they were at the end of the scan. Thus, the doses were estimated to be half of the measured dose. Estimation of red bone marrow and bone surface distribution followed the model of Hough et al. and the same doses were used for red bone marrow and bone surface (Hough et al., 2011). To estimate repeatability, the examination, including the localizer radiographs, was repeated five times with the same scanner and the same settings. The mean deviation of the TLD measurements was 0.08 mGy.

The CTDI_{vol} values from the dose display were used in study II and III to estimate the CTDI_{vol} of the different protocols and scanners. In study I and III, the DLP values were used to

estimate the effective dose by multiplying the DLP with a conversion coefficient. A value of 0.039 mSv/mGycm was used for the neonatal chest, and the DLP was multiplied with a factor of 2 if the dose was assessed with a phantom with a diameter of 32 cm (Thomas and Wang, 2008). In study III, the effective dose values were calculated by conversion factors presented by Shrimpton et al. (Shrimpton et al., 2005), which are presented in Table 2. The error of the dose display was estimated from the equipment service reports, and the difference with respect to the reference meter was less than 5.5 %. The 75th percentiles were also determined for different age groups for local DRLs. The 75th percentile was determined if there were more than ten patients in an age group.

Table 2. Conversion factors (mSv/mGycm) from DLP to effective dose (DLP measured with a 16 cm diameter phantom) (Shrimpton et al., 2005).

	0 year	1 year	5 years	10 years	Adult
Head	0.0110	0.0067	0.0040	0.0032	0.0021
Neck	0.0170	0.0120	0.0110	0.0079	0.0059

In studies IV and V, the organ doses and effective doses were calculated by the ImPACT CTDosimetry tool (excel macro made for NRPB-SR250 report by Impact group), ICRP 60 was used in study IV and ICRP 103 in study V. For dose calculation, tube voltage, current, rotation time, pitch, collimation, scan length, scan region and the model of scanner were collected for each CT examination. The manufacturer, scanner model, tube voltage and scan region (body or head) determined the used data set. Scan length and scan region were used to match the scanned region to the CTDosimetry phantom for determination of which slices, presenting normalized Monte Carlo data, should be used for dose calculation. Tube current and rotation time were needed, because the organ dose data was normalized with the tube current-rotation time product. The calculation required also CTDI-values measured in air and tabulated values founded in spreadsheet were used. The tabulated values were collimation-related. Pitch was used to consider for the possible differences between couch movement and collimation.

The data sets are made for scanners without TCM, and the dose generated by scanners utilizing tube current modulation was calculated with the mean tube current of the lowest and highest tube current-values of the scan. Scans with inadequate parameter data applied the parameters of the same scanner, similar scans covering the same body regions and IV contrast medium.

In study IV a cumulative effective dose was also determined. In this thesis a cumulative effective dose was categorized as high when it reached 50 mSv per year and a mean value of 20 mSv over 5 years (ICRP, 2007). Since there is no definition of high cumulative dose in medical exposures, this categorization was adopted from other studies on cumulative doses in medical imaging (Fazel et al., 2009; Rohner et al., 2013; Silva et al., 2012; Stiles et al., 2011).

4.5 Image quality

In studies I and II, image quality was evaluated by region of interest (ROI) measurements. In study I, ROIs were drawn in the region of the lung and heart, and the mean HUs and noise were measured. The ROI size was 250 mm² and ROIs were measured by the ROI-tool of the PACS. In study I, CNR and FOM were calculated from the measurements and CTDI_{vol} was used for the calculation of FOM. The CNR and FOM values were normalized to the results of Sensation 64 (Siemens, Erlangen, Germany). The Sensation 64 was used as a reference, because it is mainly used for pediatric imaging in our hospital.

In study II, CNR and FOM were calculated as in study I; HU and noise were also assessed for each protocol. One circular ROI was drawn in each test tube to determine the HU value and one larger ROI was drawn in the background to determine the background noise. The ROIs were drawn in each test tube at nine axial images, where the test tubes were filled with contrast material uniformly. Air bubbles were carefully avoided. CNR and FOM values were calculated for each test tube at each slice. In study II the ImageJ software version 1.49 (National Institutes of Health, Maryland, USA) was used. In study II, the test tube HU, noise, CNR, and FOM values were drawn as a function of NI for different tube voltage IR combinations and the slopes were compared to protocol E as a reference. This protocol uses 120 kVp and standard IR and it is in use in the emergency department of our hospital.

In study II, a visual image quality assessment was performed by two experienced radiologists. The radiologists were blinded to the image parameters and to the concentration of contrast material. The image quality was evaluated from each test tube on a four-point scale, where 0 = no contrast, 1 = weak, non-diagnostic contrast 2 = moderate contrast, sufficient for diagnostics and 3 = high contrast, optimal for diagnostics. These grades were further categorized as insufficient (0 and 1) and sufficient (2 and 3) for diagnostic use. From these categorized values, a cumulative number of diagnostic grades was calculated to provide a total score to evaluate protocol performance.

4.6 Statistics

In studies II, III and V statistical analysis was used. In study II, mixed models were used to compare the slopes and means of different tube voltage IR combinations (A, B, C, D and F) to the reference (E). The mixed models take both fixed and random effects into account, and are thus useful when repeated measurements are made on the same statistical units. In order to take into account the possible dependencies between the measurements from different slices, the test tubes in every image slice were used as a random effect in statistical modelling.

The tube voltage-IR combinations (A-F) were used as a categorical variable and the concentration and NI as continuous explanatory variables in the statistical model. The results

of the ROI-measurements (HU, noise, CNR and FOM) were analyzed separately. In the analysis of FOM, only concentrations over 1.5 mg/ml of iodine were analyzed. Logarithmic transformation was used to achieve a normal distribution with the second-degree term of concentration included in the model, as well. Interactions of variables, if statistically significant, were included in the statistical model.

In study III, descriptive statistics models were used, where the main statistical analyses for $CTDI_{vol}$ were performed using a mixed linear model. Relationships between $CTDI_{vol}$ and independent variables (e.g., scanner, age group, indication, scanning type (volume or spiral) and study date) were studied. The variable study date was used to indicate whether the study was performed before or after a parameter change made on 12 May 2015 or 12 November 2015. The normality of the distribution of variables were evaluated visually and tested with the Shapiro-Wilk test.

Wilcoxon's Two-Sample Test was used in study V for non-normally distributed variables to examine group differences. The SAS system for Windows, Version 9.3 (SAS Institute Inc, Cary, NC, USA) was used for statistical calculations in all studies and P-values less than 0.05 were considered statistically significant.

5 RESULTS

5.1 Radiation dose and image quality of CT studies of the chest of neonate (study I)

The measured point doses are presented in Figure 6. The effective doses calculated by TLD measurements, ImPact CT Dosimetry and DLP multiplied with coefficients for different scanners are presented in Figure 7. The effective doses were less than 1 mSv for newborn babies undergoing CT of the thorax, and only LigthSpeed 16 produced a higher dose of 1.1 mSv, when the effective dose was calculated from DLP.

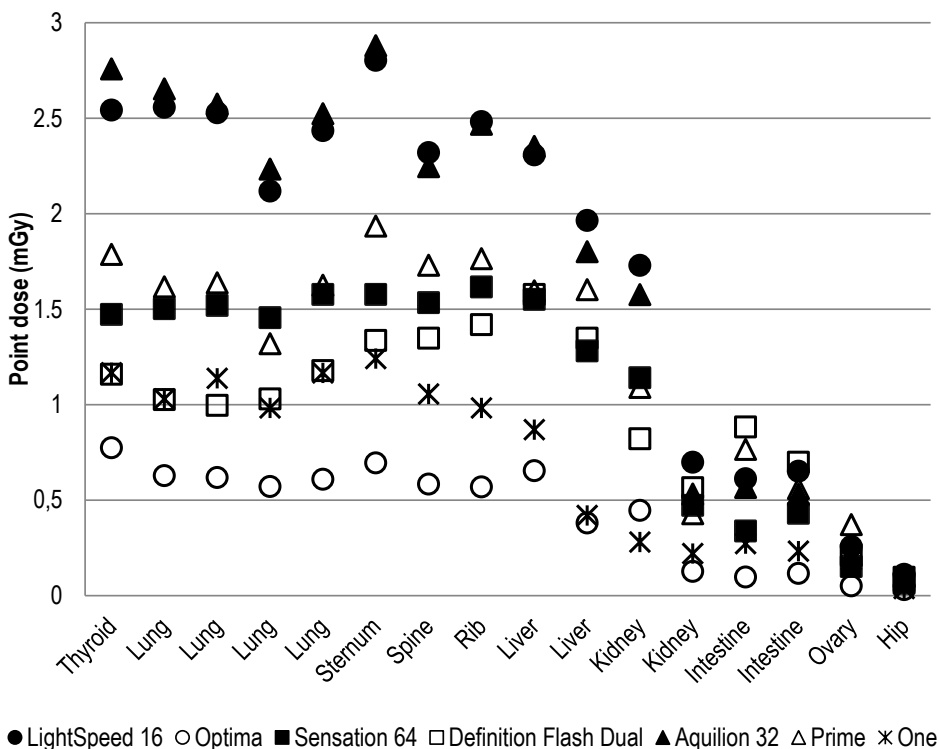


Figure 6. Measured point doses of newborn from chest CT studies. Data for all seven scanners, including localizer radiographs, are included. Modified from study I.

When the ratio of the effective dose of plain localizer radiographs and the whole study were assessed, the localizer radiographs turned out to contribute a significant percentage of the total dose. The Aquilion 32 and Aquilion Prime used two localizer radiographs, the other scanners one. The doses and percentage contribution to the total dose are presented in Figure 8.

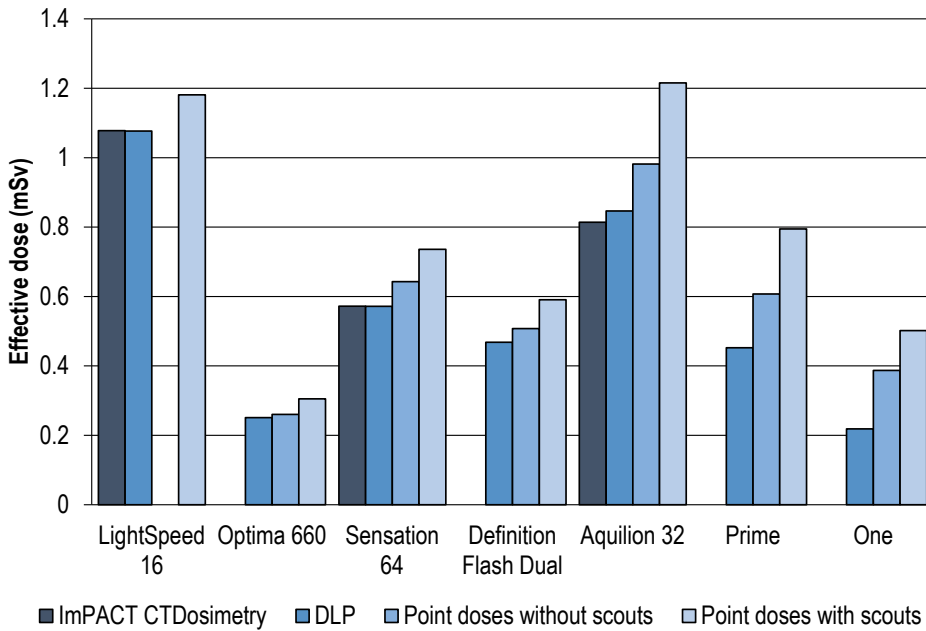


Figure 7. Effective doses from newborn chest CT studies. Data for all seven scanners calculated with different methods are shown. Modified from study I.

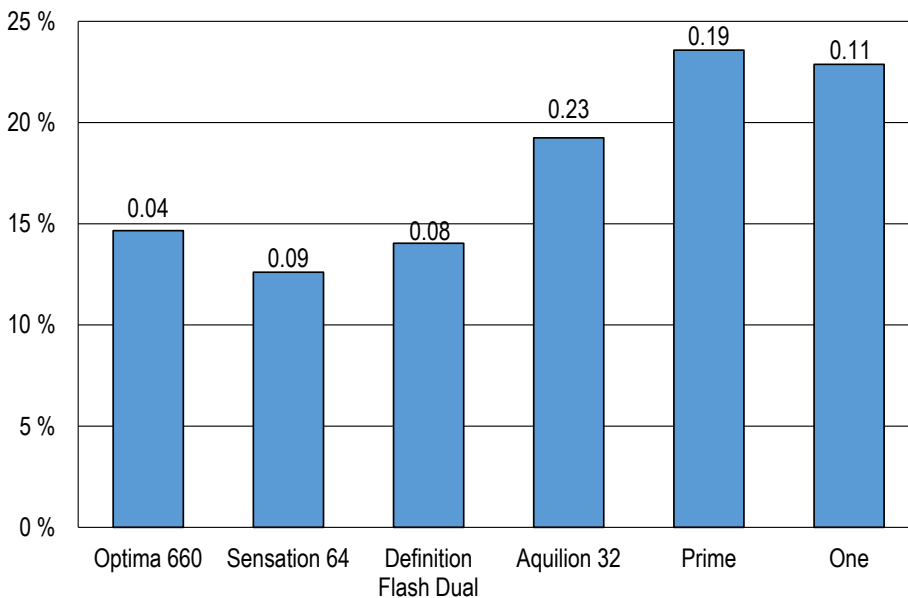


Figure 8. Percentage contribution of the localizer radiographs to the total effective dose to the newborn chest from different CT scanners. Effective doses (mSv) provided by localizer radiographs are marked above the bar. The dose of localizer radiographs could not be measured for the LightSpeed 16 device which was removed from use.

The CNR and FOM values are presented in Table 3. When assessing the CNR of different CT scanners, the scanners of older model, e.g., LightSpeed 16 and Aquilion 32, generated higher CNRs than the newer models of the same manufacturer. However, the FOM values were 16–68 % higher for the more modern scanners compared to the Sensation 64 which is used routinely. Only the Aquilion 32 achieved a 43 % lower FOM than the Sensation 64.

Table 3. Contrast to noise ratio (CNR) and figure of merit (FOM) values for all seven scanners used for pediatric chest CT in study I normalized to the values for the Sensation 64 scanner.

	Light-Speed 16	Optima 660	Sensation 64	Flash Dual	Aquilion 32	Prime	One
CNR	1.44	0.79	1.00	1.57	1.22	0.62	0.80
FOM	1.16	1.68	1.00	1.27	0.56	1.31	1.36

The scanning protocols varied widely. All of the scanners used an 80 kVp tube voltage, the rotation time was 0.5 s except for the Aquilion One and Definition Flash Dual, which used a rotation time below 0.35 s, the tube current differences were ten-fold, pitch values range from 0.813 to 3.0 and IR was not selectable in all scanners. Newer devices with two x-ray tubes or volume imaging, such as the Definition Flash and Aquilion One, provided faster imaging (scan duration was below 0.32 s), which is a valuable feature when patients may not be cooperative. The results of study I showed that the newer devices using dose-saving methods, like IR or volume scanning, generate a lower effective dose and lower point doses, and they also take advantage of the radiation for better image formation.

5.2 Optimization of abdominal CT (study II)

The HU values decreased with higher tube voltage and lower contrast concentrations, as expected, and there was no difference between the HU values on different IRs at the same tube voltage. When the measured noise was presented as a function of NI, the slopes of protocols A and B differed significantly ($p < 0.001$) from our reference protocol (E), as shown in Figure 9 A. Although A and B produced the highest noise, they also resulted in higher doses compared to other tube voltages with the same IR as in Figure 9 B.

The CNR decreased linearly with NI, and the slopes of A, B ($p < 0.001$) and C ($p = 0.002$) were significantly steeper than of the reference E, as shown in Figure 10. The decrease of CNR was more pronounced at higher concentrations.

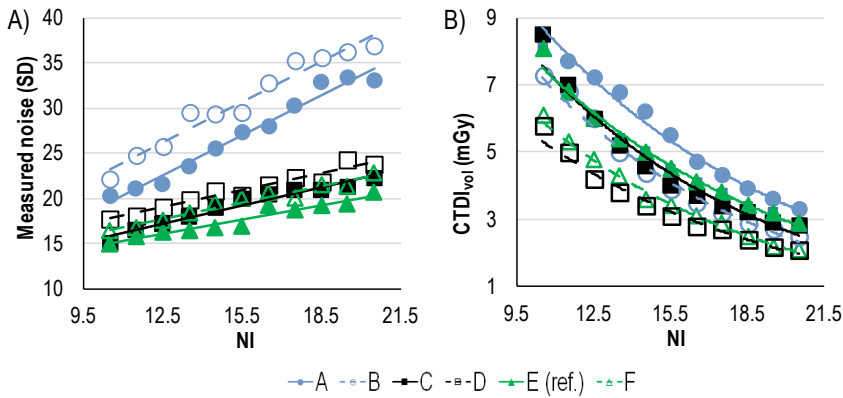


Figure 9. Noise **A)** and radiation dose **B)** for protocols A-F by noise input value (NI). Modified from study II

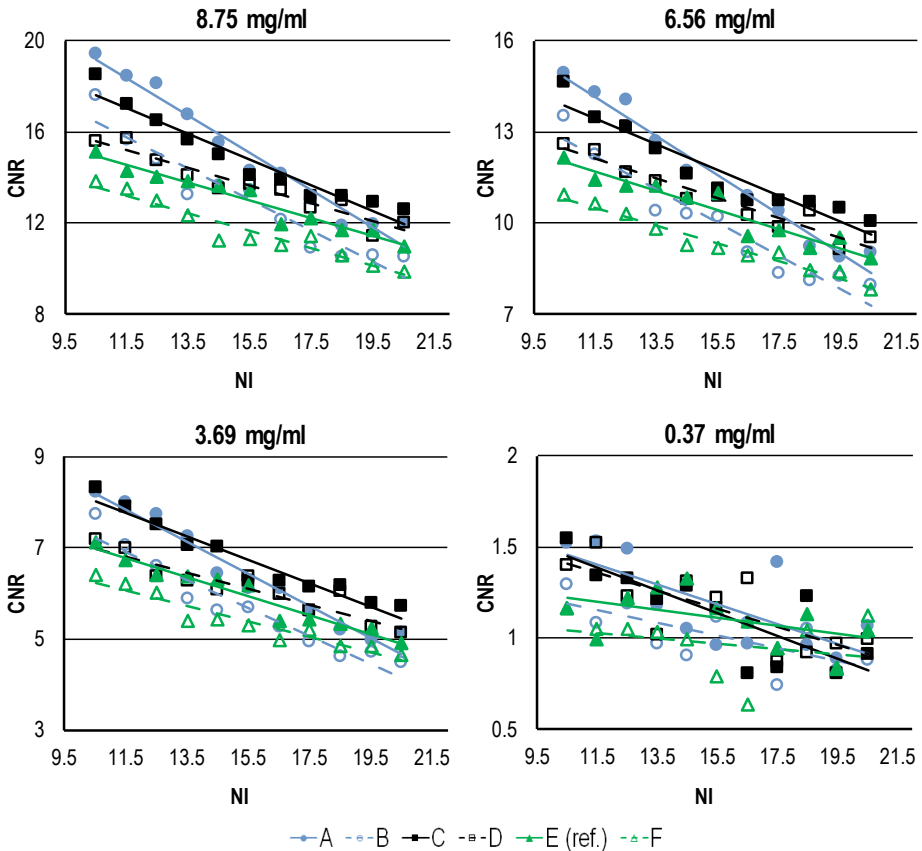


Figure 10. Contrast to noise ratio (CNR) as a function noise input value (NI) at different concentrations of contrast medium, protocols A-F. Modified from study II.

The FOM as a function of NI at different protocols are presented in Figure 11. When assessing FOM, the slopes of protocols A and B at 80 kVp differed significantly from the slope

of reference protocol E ($p < 0.001$), but there was no difference in the slopes between protocols C, D and F in comparison to the reference. Because there was no difference between the slopes of C to F in comparison to the reference, an additional analysis to these protocols was done. In this additional analysis the interaction of protocols and NI were not statistically significant in the model, and hence the interaction was expelled from the statistical model and the mean FOM values could be compared. The mean FOMs (95 % CI) of protocols C, D, E and F differed statistically significantly from each other ($p < 0.001$); the respective values were 9.17 (8.96 to 9.38), 10.50 (10.26 to 10.74), 6.84 (6.68 to 7.00) and 7.42 (7.26 to 7.59). With protocols C and D the FOM values were 15.5 % and 22.4 % higher when compared to E.

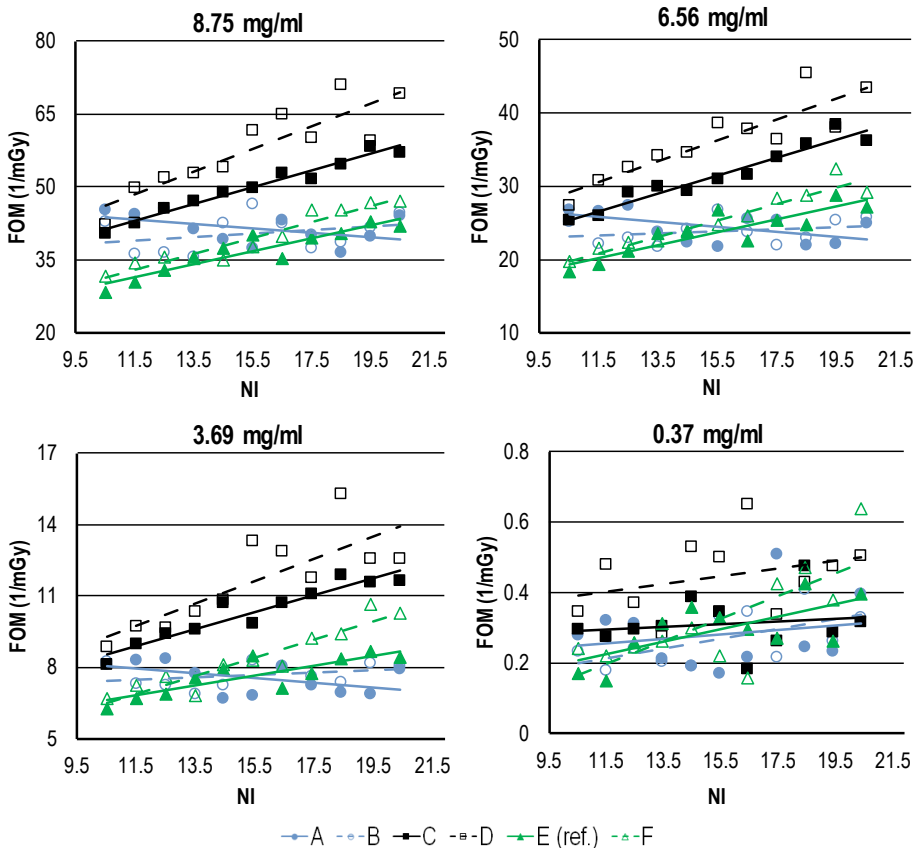


Figure 11: Figure of merit (FOM) as a function noise input value (NI) at different concentrations of contrast medium, protocols A-F. FOM illustrates the contrast to noise ratio (CNR) squared in relation to the radiation dose. Modified from study II.

The image quality scores of the visual analyses are presented in Table 4. The grades decrease with increasing NI. The standard IR achieved higher grades than the strong IR. Protocols C and E achieved the highest total score, F the lowest. The inter-reader Kappa-value was 0.76 (95 % CL 0.71 to 0.8).

Table 4. Image quality score of each protocol (A-F) by noise input (NI) value. The total image quality score calculated as a cumulative number of diagnostic grades.

NI	A)	B)	C)	D)	E)	F)
	80kVp stand IR	80 kVp strong IR	100 kVp stand IR	100 kVp strong IR	120 kVp stand IR	120 kVp strong IR
10.5	11	11	12	11	11	10
11.5	11	10	11	11	11	10
12.5	11	10	10	11	11	10
13.5	10	10	10	10	10	9
14.5	10	10	10	10	10	10
15.5	9	8	10	10	10	9
16.5	9	8	9	8	9	8
17.5	8	8	9	8	8	6
18.5	8	8	8	8	8	4
19.5	7	7	7	5	8	4
20.5	7	6	7	5	7	4
Total score	101	96	103	97	103	84

Protocols A and B using 80 kVp had significantly higher noise than protocols C-F using tube voltages of 100 kVp or 120 kVp. The protocols with 100 kVp achieved highest FOM, as they offered higher image quality with same CTDI_{vol} in contrast to 120 kVp protocols. The CNR of 100 kVp was higher with standard IR compared to strong IR. Physical measurements showed that 100 kVp with standard IR seems to be a plausible choice for further assessment. Moreover, the image quality score at 100 kVp with standard IR corresponded to the performance of the reference protocol (Table 4) and achieved a higher total visual score than strong IR. Thus, 100 kVp with standard IR is the optimal in this case. A slightly higher NI level compared to the routine NI of 12.5 could be feasible for this protocol and further *in vivo* analysis. The CTDI_{vol} at 100 kVp, standard IR and NI of 14.5 is 23 % lower when compared to the reference, which indicated that the previously used protocol may not have been fully optimized.

5.3 CTDI_{vol} and effective dose of CT studies of the head and cervical spine in the emergency department setting (study III)

The data collected with dose monitoring software revealed significant differences in CTDI_{vol} values between the two scanners (Aquilion One and Definition Dual Flash) in all indications. Protocol updating lowered the radiation dose and also un-optimized protocols were identified. Deviations of head and cervical spine CT doses are presented as a function of study date and patient age in Figure 12. In all indications, the CTDI_{vol} values increased with age, as expected, but the increase was stronger with the Definition Flash scanner in routine head ($p < 0.001$) and cervical spine ($p = 0.003$) CT studies than with the Aquilion One. The trauma head CT doses were statistically significantly higher ($p < 0.001$) than routine head CT doses on both scanners.

The mean CTDI_{vol} values were 24–62 % lower ($p < 0.001$) with the Aquilion One in all indications and also the mean scanning lengths were shorter ($p < 0.001$) than with the Denition

Flash. The mean $CTDI_{vol}$ (SD) related to trauma head, routine head and trauma cervical spine CT studies for the Aquilion One and Definition Flash were 40.3 mGy (SD 12.3 mGy), 30.0 mGy (SD 11.1 mGy), 6.9 mGy (SD 3.1 mGy) and 53.0 mGy (SD 12.9 mGy), 43.2 mGy (SD 8.7 mGy), 18.3 mGy (SD 7.3 mGy), respectively. The mean doses by age groups and the national DRLs for routine head CT are presented in Table 5. The routine head $CTDI_{vol}$ exceeded the national DRLs among patients younger than 16 years when the Definition Flash was used (STUK, 2013; STUK, 2015).

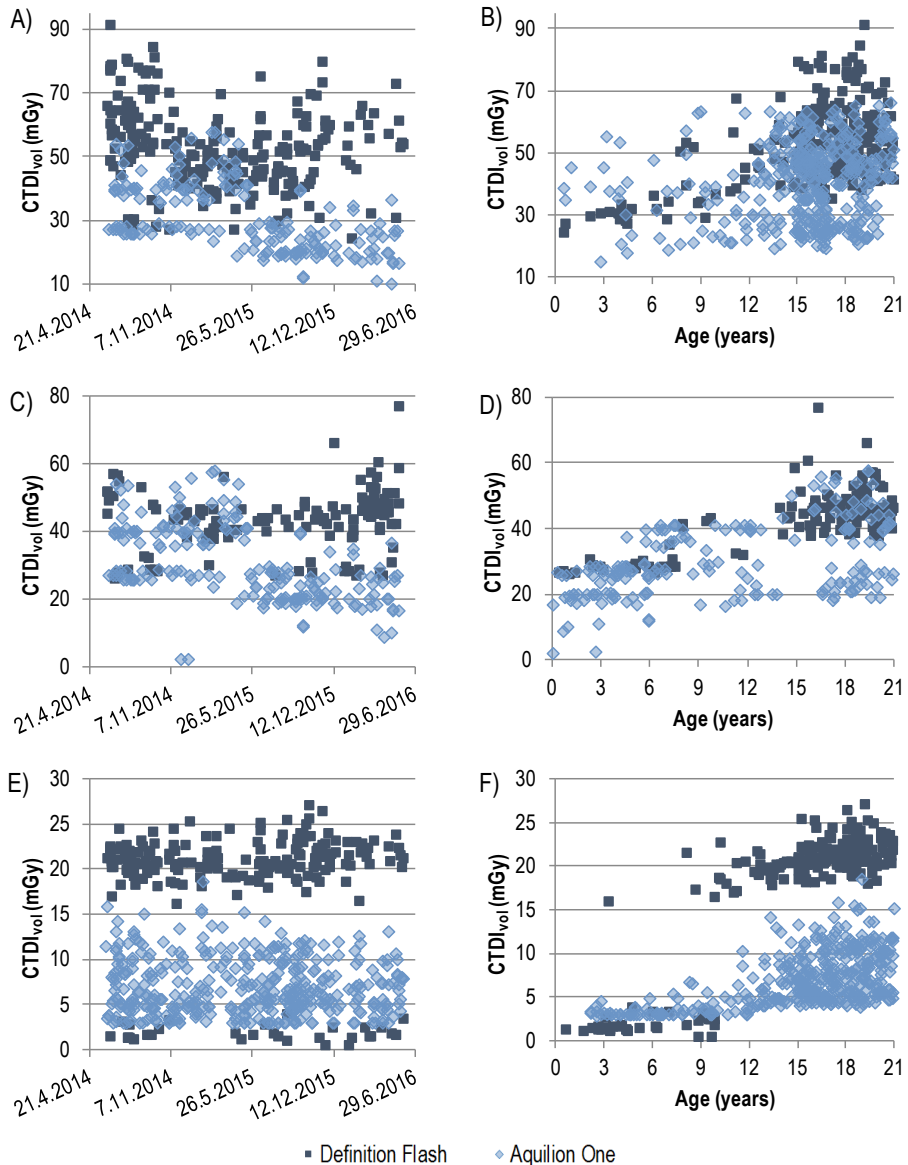


Figure 12. $CTDI_{vol}$ as a function of study date and patient age by different scanners and indications. **A)** and **B)** trauma head CT doses, **C)** and **D)** routine head CT and **E)** and **F)** trauma cervical spine.

Table 5. Mean CTDI_{vol} (SD) for different age groups with the Definition Flash and Aquilion One scanners. Only the latest protocols of the Aquilion One have been considered for estimation of mean CTDI_{vol} values. National DRLs are presented for routine head CT (STUK, 2013; STUK, 2015). Units are mGys.

		1–5 years	6–10 years	11–15 years	16–20 years
Trauma head CT	Flash	29.5 (2.5)	39.6 (9.4)	52.7 (9.8)	56.1 (12)
	One	31.9 (11.4)	30.6 (9.6)	38.9 (11.8)	4.14 (12.4)
Routine head CT	Flash	28.1 (1.3)	33.9 (6.7)	43.6 (7.7)	46.8 (6.0)
	One*	19.0 (4.5)	29.0 (6.6)	21.1 (2.8)	24.8 (5.3)
	DRL	25	29	35	55
Cervical spine CT	Flash	2.4 (3.4)	8.2 (8.4)	20.6 (1.5)	21.8 (2.4)
	One	3.3 (0.5)	3.7 (1.0)	6.6 (2.3)	8.2 (3.0)

* Volume scanning was used for studying patients under 16 years old, otherwise helical scanning was used.

The CTDI_{vol} was significantly ($p < 0.001$) reduced when the head CT protocol parameters of the Aquilion One were changed from standard to strong IR and the NI concomitantly increased from 2.3 to 3.0. The mean CTDI_{vol} decreased from 50.4 mGy (SD 7.2 mGy) to 30.0 mGy (SD 7.8 mGy) in the trauma head protocol and from 36.9 mGy (SD 10.5 mGy) to 23.0 mGy (SD 6.3 mGy) in the routine head protocol. As seen in Figure 12 A) and C), the level of CTDI_{vol} dropped on May 2015. Later on, in November 2015 the trauma head dose increased ($p = 0.04$) to 32.5 mGy (SD 7.5 mGy), when the NI was decreased to 2.8. The total reduction of the mean CTDI_{vol} in the trauma head protocol from 50.4 mGy to 32.5 mGy was no less than 35.5 %.

The mean effective doses were below 6 mSv in all studies, age groups and both scanners (Fig. 13). There was no correlation between age and effective dose, although there was a statistical difference between the effective doses of age groups ($p = 0.009$). The radiation dose correlated with CTDI_{vol}; the dose increased with age, but when the effective dose was calculated, the conversion factors correspondingly decreased with age. The mean effective doses of trauma head are of similar magnitude in all age groups, as the maximum difference of the mean effective dose was 0.6 mSv in all age groups except the youngest group examined with the Aquilion One. The effective doses were higher for a limited number of patients (4) who had high CTDI_{vol} values. An un-optimized practice emerged with the use of the Definition Flash scanner: the dose increased abruptly for patients aged above 10 years (Fig. 12 F) when the adult protocol was applied. This was also the case for effective doses (Fig. 13). The deviation in age group 6–10 years scanned with the Definition Flash was wide and high in age groups 11–15 years and 16–20 years. The CTDI_{vol} varied also widely among patients above 10 years of age who were scanned with the Aquilion One, but the increase in mean CTDI_{vol} was moderate and probably due to the normal variation of patient size.

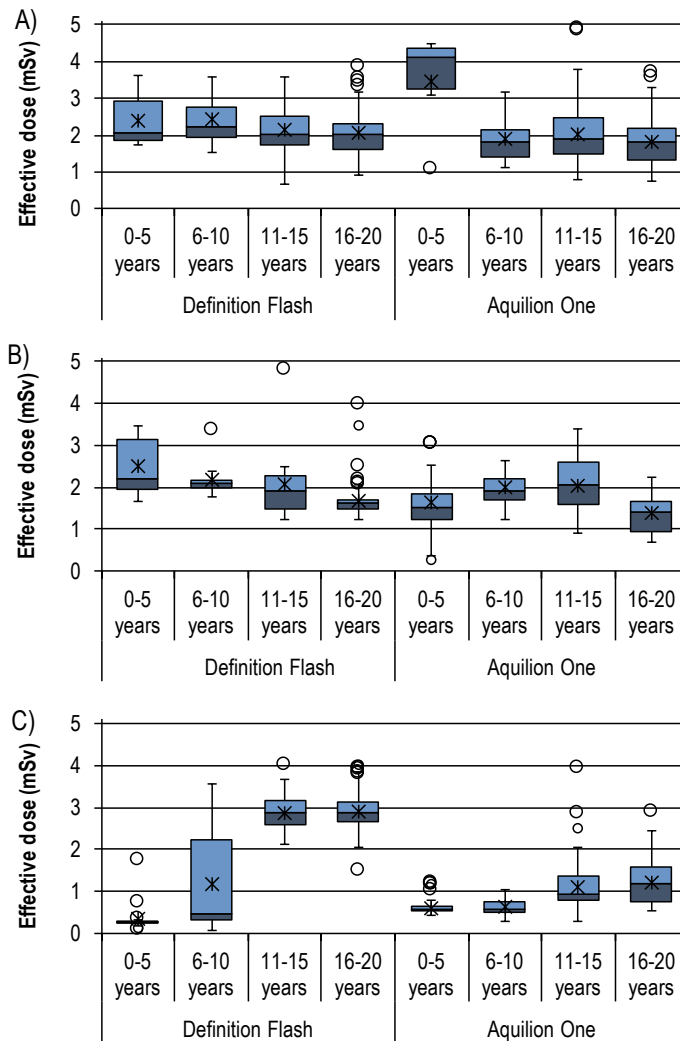


Figure 13. Effective dose for trauma head (A), routine head (B) and trauma cervical spine (C) CT. Mean values are presented with asterisks, median is the line inside the box and the upper and lower hinge of the box show the 75th and 25th percentiles, respectively. The whiskers show minimum and maximum values and circles outliers. The point is an outlier, if the value is 3/2 times higher or lower than the hinges.

The 75th percentiles were also determined from the dose data. The percentiles for the different indications are presented in Table 6. The 75th percentiles of trauma and routine head cannot be considered as local DRLs, because the percentiles of routine head at both hospitals exceed the national DRLs (STUK, 2013; STUK, 2015). The percentiles of the trauma head CT were also a slightly higher with the Denition Flash, when percentiles were compared with other national DRLs (Buls et al., 2010; Jackson et al., 2015; Shrimpton et al., 2014; Verdun et al., 2008). With the Aquilion One, there were less than 10 patients in the youngest age group undergoing head trauma CT which precluded DRL calculations. The 75th $CTDI_{vol}$ percentile from cervical spine CTs can be set as local DRLs.

Table 6. 75th percentiles of CTDI_{vol} (mGy) with the Definition Flash and Aquilion One scanners for different age groups. In the trauma head CT group, only the updated head protocol was considered for the Aquilion One.

		1–5 years	6–10 years	11–15 years	16–20 years
Trauma head CT	Flash	30.8	50.4	57.0	62.9
	One			39.5	39.6
Routine head CT	Flash	28.8	40.9	46.6	48.6
	One*	21.7	39.5	40.6	26.9
Cervical spine CT	Flash	1.6	17.3	20.8	22.8
	One	3.3	3.8	7.9	10.5

*Volume scanning was used for patients younger than 16 years and helical scanning for older patients.

5.4 Organ doses and cumulative effective doses from CT screening of testicular cancer (study IV)

The mean number of CT studies per patient was six, and the maximum was 26 studies on one patient. Fifteen different CT scanners used, but 94 % of the examinations were made with six scanners. Table 7 shows the minimum and maximum organ doses and effective doses from CT scans of the abdomen and the whole body. Although the indication and patient group were the same, there was at maximum a nine-fold difference in organ doses. The highest dose of 65 mGy was received by the liver, the lowest by the lenses, which are not included in the scan area. In terms of effective dose, a maximum six-fold difference was observed between the minimum and maximum dose.

Table 7. Minimum and maximum organ doses (mGy) and effective dose (mSv) to patients with testicular cancer from different CT examinations made during follow-up.

Organ	Abdomen nat ^a	Abdomen IV ^b	Abdomen nat+IV	WB ^c nat	WB IV	WB nat+IV
Lungs	1.0–12	1.3–14	1.8–19	7.5–34	6.6–36	6.8–42
Stomach	1.0–26	7.4–32	6.9–51	6.9–31	5.9–38	7.8–51
Bladder	4.8–31	5.4–30	6.4–30	6.5–30	5.2–32	4.0–36
Breast	0.3–7.2	0.4–7.8	0.6–15	6.5–30	1.7–30	3.7–31
Liver	7.0–25	7.2–31	7.0–49	7.0–31	6.0–37	7.9–65
Red bone marrow	2.9–13	3.0–11	4.1–17	4.5–21	4.1–21	3.9–27
Testicles	0.3–26	0.4–26	0.1–27	0.5–26	0.4–28	0.11–26
Colon	4.8–24	4.8–31	5.6–31	5.1–27	4.5–26	3.8–27
Lens	0	0–0.07	0–0.09	0.04–0.5	0–0.01	0.03–3.6
Heart	1.0–18	1.3–16	1.8–22	6.7–31	5.8–36	5.7–40
Pancreas	6.4–26	6.6–30	6.5–49	6.5–29	5.5–36	7.2–62
Effective dose	3.6–18	3.7–16	5.6–23	5.3–26	5.1–21	6–36

^a without IV contrast enhancement

^b with IV contrast enhancement

^c WB=Whole body

Frequent CT studies led to relatively high cumulative effective doses. The highest cumulative dose was 282 mSv. In this study 24 % of the patients were subjected to more than 50 mSv in one year and 5 % of patients reached a 5-years mean of 20 mSv. The variation of cumulative effective doses in this patient group is presented in Figure 14.

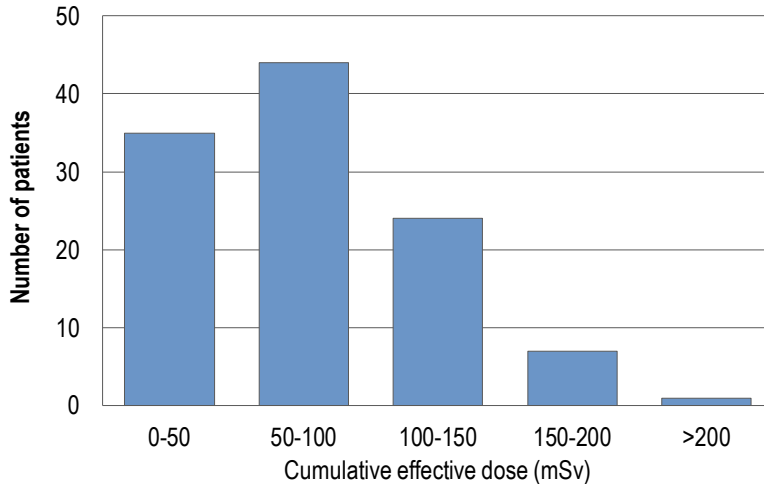


Figure 14. Variation of cumulative effective doses to patients testicular cancer during follow-up. Reprinted from study IV.

5.5 Effect of CT scanner and IV contrast agent on radiation dose (study V)

In study V, the effective dose resulting from a whole body CT study of patients with testicular cancer was, on average, 7 mSv for the Plus 4 scanner and 12 mSv for the LightSpeed 16 scanner. Figure 15 shows a box plot of effective doses of both scanners, and the higher doses of the LightSpeed 16 are obvious. The doses from both scanners, with and without IV contrast and with patients of different size (waist circumference) are presented in Table 8.

Table 8. Effective doses (SD) with intravenous (IV) and without IV contrast medium generated by two CT scanners. The number of studies among patients with a waist circumference below and above 100 cm are presented in parenthesis.

	LightSpeed 16		Plus 4	
	<100 cm (94)	≥ 100 cm (43)	<100 cm (116)	≥ 100 cm (26)
With IV	13.6 (3.2)	17.5 (6.1)	7.4 (1.2)	8.5 (3.3)
Without IV	10.7 (2.0)	12.8 (1.9)	6.2 (0.5)	7.7 (2.5)
All	12.8 (3.2)	16.7 (5.9)	7.2 (1.2)	8.2 (3.0)

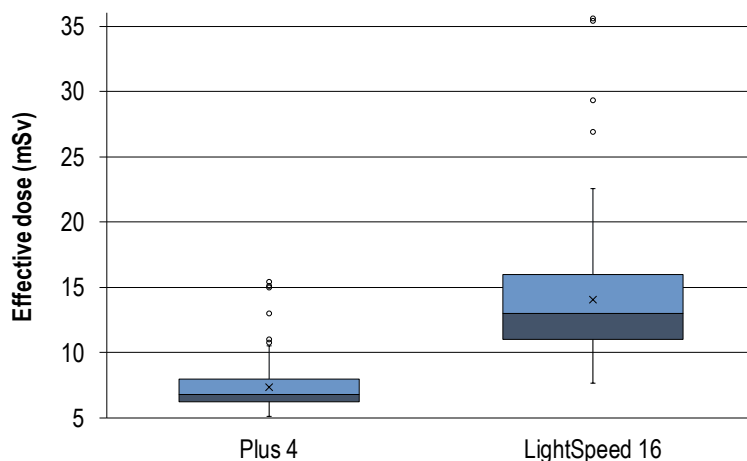


Figure 15: Box plot to show effective doses from two CT scanners. Mean values are presented with an asterisk, the median is the line inside the box and the upper and lower hinge of the box show the 75th and 25th percentile, respectively. Whiskers show minimum and maximum values and circles outliers. The point is an outlier, if the value is 3/2 times higher or lower than the hinges. Reprinted from study V.

The radiation doses were significantly lower ($p < 0.001$) for patients who were scanned with the Plus 4 scanner than with the LightSpeed 16, although the LightSpeed 16 utilized TCM. The exposure varied, as expected, with patient size: smaller patients were subjected to lower radiation doses than larger patients. The difference was statistically significant for both scanners ($p < 0.001$). The mean effective doses from the LightSpeed 16 were 12.8 mSv (SD 3.2 mSv) and 16.7 mSv (SD 5.9 mSv) and for the Plus 4 7.2 mSv (SD 1.2 mSv) and 8.2 mSv (SD 3.0 mSv) for waist circumferences below 100 cm and above 100 cm, respectively. The doses from the LightSpeed 16 were higher than the doses from the Plus 4 mainly because the LightSpeed 16 used a higher current. The current was close to 150 mA for the Plus 4 and between 53 and 441 mA for the LightSpeed 16 whose baseline was also higher. The maximum current of the scanner was used for patients with a waist circumference of 118 cm or higher. For these patients a non-modulating tube current was used, but in some cases the rotation time was increased. For larger patients, the effective dose increased proportionately more with the LightSpeed 16 than the Plus 4. Since both scanners were used for diagnostics, it is plausible that optimization was not successful with the novel LightSpeed 16 scanner which generated significantly higher doses than the older Plus 4.

When IV contrast agent was used, the radiation dose to patients increased significantly for both scanners ($p = 0.003$). The reasons for higher effective doses when IV contrast medium is used are the number of phases required for the CT study. The IV study was mostly biphasic when the Plus 4 was used and triphasic with LightSpeed 16, which increased the radiation dose compared the same study made without IV.

6 DISCUSSION

6.1 Effective dose

The effective dose was estimated in studies I and III–V because it is related to the detrimental effects of radiation and the effective dose is a means to transform exposure into equivalent uniform whole body exposure and comparison of different modalities, techniques or protocols is possible (ICRP, 2007; ICRU, 2005). However, there are some limitations regarding the determination of effective dose, which should be considered. Effective dose is calculated from the absorbed doses to organs by using weighting factors, which consider the quality of radiation and the sensitivity of organs or tissues to radiation. These weighting factors are given by the ICRP and they have been updated twice since 1977, in 1991 and in 2007 (ICRP, 1977; ICRP, 1999; ICRP, 2007). The main difference with the latest updates compared to previous ones was that the tissue weighting factor of breast tissue increased from 0.05 to 0.12 and the tissue weighting factor of the gonads decreased from 0.20 to 0.08. Boetticher has shown that the latest coefficient update has increased the effective dose to the chest CT by 21 % (Boetticher et al., 2008) and for whole body examinations the change is almost 20 %, since most radiosensitive organs are subject to irradiation (Martin, 2007b).

The weighting factors are derived from data on Japanese atomic bomb survivors. The cohort included adults of both genders, and their whole body was exposed to radiation. This is not the case when evaluating the dose from diagnostic imaging, where only a part of the body is exposed to radiation, the gender is known and the age range is wide. With CT imaging, the exposure is focused only on a certain body part and exposure is inhomogeneous during the scan because of the TCM. This can cause a situation where the effective dose is low although the equivalent dose for a specific body part is high. As effective dose is a radiation protection quantity, it is practical to have only one value, although separate guidelines ought to be considered, since women are more sensitive to radiation than men. The tissue weighting factors are averaged for both gender and ages and thus determine the effective dose for a reference patient (ICRP, 2007). The determination of effective dose is more problematic for pediatric patients, because the tissue weighting factors are independent of age, although the radiation risks are related to age. The risk for radiation-induced cancer later in life varies depending on the age at exposure. The tissue weighting factors are not related to the real risk of detrimental effects to pediatric patients. Effective dose does not consider this variation, and effective dose may underestimate the risk of detrimental effects for pediatric patients by a factor ranging from 1.5 to 4 (Brenner, 2008; Pradhan et al., 2012).

6.2 Radiation dose estimation in CT

6.2.1 $CTDI_{vol}$ and DLP

The dose display quantities ($CTDI_{vol}$ and DLP) were used to estimate the radiation doses in studies I–III. The use of $CTDI_{vol}$ and DLP has some limitations, because the $CTDI_{vol}$ is determined as the absorbed dose measured with a 100 mm ionization chamber. The 100 mm ionization chamber underestimates the air kerma-length product, especially for collimations wider than 40 mm, because the tails of scattered radiation are not included in the measurement since the chamber length is limited (Boone, 2007). The collimation of novel scanners can exceed 160 mm. With collimation of 160 mm, the 100 mm ionization chamber measures only 51 % of the $CTDI_w$, compared to the dose measured with a 300 mm ionization chamber in a 350 mm long head phantom (Geleijns et al., 2009). The IEC has still established the 100 mm ionization chamber to be used with wide collimations. The determination has been updated for collimations wider than the length of the ionization chamber, where the length of the ionization chamber is used to determine CTDI instead of NT (see equation 5) (IEC, 2009).

The Aquilion One utilized volume scanning with 100 mm collimation in studies I and III, and hence the $CTDI_{vol}$ and DLP were lower than measured. When comparing the effective dose calculated from phantom measurements without a localizer radiograph and the effective dose from DLP, there was a 77 % difference in study I. If the $CTDI_{vol}$ is underestimated by 51%, the difference in effective doses determined with these different methods would decrease to 11 %. In study III, volume scanning was used only in routine head CTs for patients under 16 years of age. The $CTDI_{vol}$ values of routine head were now below the national DRLs, but the underestimation of $CTDI_{vol}$ may have impact on the mean $CTDI_{vol}$ doses. There is a need for more uniform expression of scanner output estimation independent of collimation.

The dose display values have some uncertainty and they should be compared to measurements performed with a calibrated reference meter. In studies, I and III the dose displays values were compared to the reference measurements performed by equipment service and the difference was less than 5.4 %. This uncertainty was not taken into account in studies I and III, because it was relatively low and would not change substantially the results. In study II, the uncertainty was not considered, since the $CTDI_{vol}$ values of the same scanner were compared among themselves and uncertainty was the same in all values.

$CTDI_{vol}$ and DLP values refer to the scanner output and the quantities are reported either for a head or body phantom. The phantoms do not reflect the size or composition of real patients and these quantities are not patient doses (McCullough et al., 2011). For patient dose estimation, organ doses and E are used, although the evaluation of E or organ doses is not straightforward, because they are not measurable *in vivo*. The organ and effective doses can be estimated by suitable calculation software (studies I, IV and V), by phantom

and dosimeters (study I) or by calculating the E from DLP (studies I and III). A new term, size-specific dose estimate (SSDE) was developed to compensate for the $CTDI_{vol}$ not considering patient size. $CTDI_{vol}$ underestimates the dose to pediatric patients and small adults, because the x-ray beam is attenuated to a greater extent in large patients than in small patients when the same imaging technique is used (Nickoloff et al., 2003). SSDE is calculated by multiplying $CTDI_{vol}$ with a coefficient determined by the size of the patient described by AP/LAT width or by the effective diameter as the American Association of Physicist in Medicine presents (AAPM, 2011). The use of SSDE has not been very widespread, because CT scanners do not routinely represent SSDE together with $CTDI_{vol}$ and DLP. For organ dose estimation, a novel method has been introduced, which is based on the fact that SSDE correlates with the organ dose, if the organ is fully covered within the scan volume (Moore et al., 2014; Tian et al., 2015).

In this thesis the SSDE was not used. In study I and II, the dose was determined for standard sized phantoms, when use of the SSDE did not offer additional information compared to $CTDI_{vol}$. In study II, the $CTDI_{vol}$ was sufficient for comparing the phantom doses of different protocols as the phantom size was constant. In studies III, IV and V, the SSDE could have been used, but measuring of the AP and LAT width in all studies included in study III, IV and V was considered to be too laborious when compared to the new information achieved. The SSDE values could not be used to compare to the DRLs of Finland with those of other countries, since DRLs are given in $CTDI_{vol}$ values and DLPs.

The estimation of E from DLP is done by specific conversion coefficients, where conversion coefficients are determined as a ratio between effective dose calculated by Monte Carlo simulations and DLP for different anatomic regions (Deak et al., 2010; Huda et al., 2011; Shrimpton et al., 2005). The estimation of effective dose from DLP and conversion coefficients is problematic, since dose display values have inherent uncertainty and as the conversion coefficients are applicable in restricted situations only. The conversion coefficients may account for age, but usually not for TCM, gender, variation in body shape or size or for scanner-dependent variables, like tube voltage or filter. Gender has been shown to have a significant effect on conversion factors in CT studies of the chest and pelvis regions, but not the head (Deak et al., 2010).

The conversion factors of Shrimpton were used in studies I and III but the effective dose depends significantly on the conversion factors used. The conversion factors for newborns presented by Deak and Alessio are 0.0739 mGycm/mSv and 0.057 mGycm/mSv, which are much higher than the used 0.039 mGycm/mSv which were used (Alessio and Phillips, 2010; Deak et al., 2010). However, the difference between the effective doses estimated from DLP and ImPACT CT Dosimetry in study I was at most 4.0 %. In spite of substantial uncertainties, the conversion coefficients have turned out to be a robust tool for use in clinical practice, since they are reliable when used with large sets of data and easy to use.

6.2.2 Phantoms and TLDs

Organ doses and image quality can be estimated with the aid of specific phantoms and TLDs. In studies I and II, anthropomorphic phantoms were used, which correspond to standard sized adults or newborns of both genders. When determining organ doses with phantoms and TLDs, multiple factors affect uncertainty, *e.g.*, energy response and geometry (IAEA, 2007). The used material LiF:Mg,Cu,P has a tissue equivalent atomic number ($Z_{\text{eff}}=8.3$). The dosimeter absorbs energy similarly like patients and the material is sensitive and has good energy response at diagnostic energies. The energy response deviates at maximum by 15 % at energies between 15 keV and 10 MeV and a relative energy response compared to ionization chamber measurements and Monte Carlo simulations decreases from 40 keV to 100 keV (Carinou et al., 2008; Duggan et al., 2004; Hranitzky et al., 2006). Because the filtration differs between scanners and this influences the photon energies, the energy response of TLDs may vary for different scanners (study I). The energy response may have had a slight effect on the organ dose measurements.

The uncertainty caused by measurement geometry arises from phantom placement with respect to the isocenter and TLD placement in phantom. When comparing different CT scanners, the positioning of the phantom should be similar in all measurements because off-centering affects the dose by TCM and bow tie filters. Kaasalainen et al. have shown 12 % higher and 8 % lower CTDI_{vol} values in newborn chest CT studies, when the phantom was positioned 6 cm below or above the isocenter, respectively (Kaasalainen et al., 2013). The measured dose is also dependent on TLD placement, because the TLDs should be positioned exactly in the same positions in the phantom so that point doses are comparable. There was some fluctuation in geometry in study I, because the scan start angle of the x-ray tube and pitch differed between scanners.

The use of point doses limits the accuracy of organ and thus of effective dose determinations. With phantom measurements, the number of TLDs is limited and places for TLDs are restricted to certain locations. The TLDs only represent absorbed dose in one specific point, which affects the accuracy of tissue and organ dose measurements. Cakmak and Groves have compared the organ doses and effective dose determined with CT Dosimetry and TLD ships. Both used Rando Alderson phantom, Cakmak used two TLDs per organ and Groves three. In Cakmak's study the maximum difference was observed in kidney, where TLDs showed 3.5 times higher organ doses than CT Dosimetry and the difference in organ doses between the methods varied from -19 % to 32% in different scan region. In Groves study the maximum difference was in the breast, where TLDs showed a 1.75 times higher organ dose and an 18% higher effective dose when determined with TLDs (Cakmak et al., 2015; Groves et al., 2004). Similar results were observed in study I: TLD measurements showed 12 % and 21 % higher effective doses than CT Dosimetry from Sensation 64 and Aquilion 32 scanners, respectively. In study I, a repeatability test was also performed, and a mean deviation of 0.08 mGy was found. This limits the reliability of the lowest point doses measured especially outside the scan region, since the measured deviation is higher than the

lowest absorbed doses measured. In the scan area, the point doses are higher and the deviation is lower than measured point doses. Nevertheless, the required accuracy of 30–50 % for low organ doses was presumably achieved (ICRU, 2005).

Organ doses can be measured with radiophotoluminescent dosimeters (RPLD) or metal-oxide-semiconductor field effect transistors (MOSFET) rather than TLDs. The use of RPLDs is similar to TLDs: both annealing and readout and both are time-consuming in use. For further phantom studies, the MOSFET would be a preferable choice, as it is accurate and provides a direct read out of real time measurements (Yoshizumi et al., 2007).

6.2.3 *ImPact CTDosimetry*

With the use of ImPACT CTDosimetry uncertainties arise from the used phantom, the measurements made for scanner output modelling, Monte Carlo simulations, datasets and the lack of TCM in calculations. Jansen and Shrimpton have made new Monte Carlo simulations for three old scanners originally used in ImPACT CTDosimetry and one newer scanner to estimate the quality of the original simulations and the reliability of the used ImPACT factor. These results showed similar effective and organ doses as for old scanners at both simulations, where the relative differences between simulations for all organs were below 5 % and the relative standard deviation for the effective dose was 1.8 %. For the newer scanner, the simulations were comparable for tube voltages 100 kVp and 120 kVp and the mean relative difference was at most 3.0 %. This study provides reliability for the use of CTDosimetry and ImPACT factors (Jansen and Shrimpton, 2016).

CTDosimetry utilizes a Medical Internal Radiation Dosimetry phantom corresponding to a standard adult and organs are represented with mathematical equations and geometric forms. More sophisticated phantoms, such as voxelized phantoms, have been developed with the use of MRI or CT scans of real patients. The voxelized phantoms function as reference males and reference females and they are recommended for evaluation of effective doses by the ICRP (ICRP, 2009). When the organ doses and effective doses determined with ICRP 110 phantoms and the Monte Carlo program made at Duke University were compared to CTDosimetry, differences ranging from 13 to 37 % were recorded for fully irradiated organs. The difference resulted from differently sized and placed organs in phantoms. When organ doses calculated with CTDosimetry were compared to organ doses calculated with hybrid phantoms, the differences were significant in organs near the scan boundary. The doses were calculated for multiple studies with both phantoms and the liver doses of CTDosimetry were at most 0.4 times lower or 10 times higher than with hybrid phantoms in the abdominal region. The difference was due to the placement of organs in the phantoms in relation to scan start and length; organ doses deviated more when the scan was of short length (Bahadori et al., 2015).

Although old, the CTDosimetry spreadsheet seems to result in organ doses comparable with other Monte Carlo calculations and phantoms. However, the major issue related to

phantoms used in organ dose calculations and TLD measurements is that they do not correspond to the variation of patients' sizes. Ding et al. estimated the difference in organ doses between anatomically realistic phantoms and CTdosimetry phantoms with the same scan settings. Because adipose tissue shields the radiosensitive organs in body, organ doses are lower with phantoms simulating morbidly obese patients. The maximum difference between phantom measurements was observed in the urinary bladder, where the organ dose was estimated to be 1.5 times lower for the morbidly obese phantom (Ding et al., 2015). When the percentages presented by Ding were used in CTdosimetry in study V, the effective dose decreased by 31 % in whole body CT studies of the largest patient. The marked differences between organ and effective doses in studies IV and V would have been lower patient size been considered. However, morbidly obese patients comprise only a minority of patients in cohort and the discrepancy would decrease when the patient size decreases towards normal BMI.

6.3 Study related risk

Magnetic resonance imaging (MRI) is more recommendable for pediatric patients than CT as it does not use ionizing radiation. However, MRI studies are time consuming and sedation or general anesthesia is needed and anesthesia may cause adverse events (Metzner et al., 2009). On the other hand, some studies have shown DNA double-strand breaks (DSBs) in MRI studies. These DSBs occur in heart imaging, where fast gradients are used, and thus these effects may not take place with shorter gradients or pediatric populations (Fiechter et al., 2013; Jaffer and Murphy, 2017; Khursheed et al., 2002). According to study I, the point doses ranged from 0.03 to 2.9 mGy for the newborn chest CT. Although pediatric patients are more sensitive to radiation than adults, the dose is low and the risk for radiation-induced cancer from one study can be assumed to be low. CT studies are also fast, as shown in study I where the duration of the fastest scan was below one second. The short duration of the study reduces the need for sedation. Clearly, the decision between CT and MRI should be considered carefully. Since there was a lack of small children in study III despite the two-year data collection period, it can be assumed that they were imaged with MRI in our hospital.

Study IV showed that patients with testicular cancer are subject to high cumulative effective doses. A large variation in effective doses for cancer follow-up has also been reported by Calandrino et al. and high cumulative doses related to follow-up of testicular cancer by Silva et al. (Calandrino et al., 2013; Silva et al., 2012). Within the cohort 61.7 % received a 50 mSv or higher cumulative dose during a 1-year period and 32 % exceeded the 20 mSv per year in five years of follow-up (Silva et al., 2012). In study IV the percentages were slightly lower: 24 % and 5 %, respectively. Tarin et al. estimated the risk associated with radiation exposure from CT imaging in the follow-up of testicular cancer and suggest that the lifetime attributable risk of secondary cancer for the AYA group is 1.23 % –1.93% depending on

age (Tarin et al., 2009). In a study by Salminen et al. the risk for radiation related cancer deaths calculated by the UNSCEAR model was estimated to be 2 % from CT examinations of follow-up for testicular cancer patients (Salminen et al., 2017). The effectiveness of clinical follow-up which includes imaging has been debated due to this risk and due to suboptimal clinical performance in identifying malignant disease during follow-up. In a study by Buchler et al. 27 % of the second tumors were detected by preplanned oncology follow-up investigations and the rest by nononcology physicians (19 %) or the patients themselves (54 %). When assessing the follow-up CTs made within six months prior to the diagnosis of the second cancer, 71 % of CT scans were negative (Buchler et al., 2011). Because of the demonstrated high cumulative effective doses and relatively low effectiveness of follow-up, the overall justification of follow-up studies should be considered more specifically in the future.

The use of IV contrast agent may cause adverse effect like allergic reactions or nephrotoxicity, but it has also been shown to increase the number of peripheral lymphocyte DNA DSBs (Beckett et al., 2015; de Gonzalez and Kleinerman, 2015; Deinzer et al., 2014; Piechowiak et al., 2015). These lymphocyte DNA DSBs have also been used in short-term accidents and long-term occupational exposures to estimate the influence of radiation, and the number of DSBs has been linked to cancer risk in epidemiological studies (Bonassi et al., 2008; de Gonzalez and Kleinerman, 2015). The use of IV contrast may increase the cancer risk, since the use of IV contrast agent increases the number of DSBs of DNA, but also because the radiation dose is higher when IV contrast agents are involved as also observed in study V. The doses were at maximum 37 % higher in contrast-enhanced studies than non-enhanced studies in the group of larger patients, who were scanned with Light-Speed 16. The main reason for the difference of effective doses between studies with and without IV is the number of phases. As the increase is significant, the number of phases should be considered with care and related to diagnostic benefit.

Fält et al. have proposed to balance the amount of IV contrast agent and the radiation dose to reduce the combined age-specific risk: lower radiation doses and higher amounts of IV contrast agent could be suitable for younger patients and *vice versa* for older patients (Fält et al., 2013). This method may be questionable, since higher amount of IV contrast medium increases the number of DSBs, which, in turn, may raise the risk of secondary cancers risk for young patients. For now, the benefits of using IV contrast agents override the harmful effects.

6.4 Optimization

This thesis shows that there is a wide variation in CT doses which is independent of the type of study population, and that follow-up CT studies of patients treated for testicular are numerous and subject the patients to high cumulative effective doses of radiation. In study

I, the mean effective doses determined from DLP to the newborn chest CT ranged from 0.22 to 1.1 mSv, *i.e.*, a five-fold difference in effective dose. In study II, phantom optimization suggests that the radiation dose generated by CT studies of the abdomen for examine acute appendicitis could be reduced by approximately 20 %–25 %. In study III, the $CTDI_{vol}$ of trauma cervical spine CT studies showed three-fold maximum dose variations and head CT two-fold maximum dose variations for identical indications and age groups. Marked differences were also observed in studies IV and V, where a maximum of nine-fold difference was observed regarding organ doses and a six-fold difference regarding effective doses. Of note, the effect of patient size was not taken into consideration for these calculations. Rather, the variation was due to variations in scanners, protocol parameters and the use of IV contrast agent.

The large variations in radiation doses and high cumulative effective doses emphasize the need for careful parameter setting, harmonization and dose monitoring as efforts to identify non-optimized protocols. In study III, dose monitoring software revealed a non-optimized protocol, where an adult protocol was used to study children from age 10 years. De Bondt et al. have reported similar results, where dose monitoring software showed that several pediatric head CT studies had been performed erroneously with an adult protocol (Bondt et al., 2016). In study V, the current level of the LightSpeed 16 was unnecessarily high. The dose for the standard sized patient was below the national DRL ($CTDI_{vol}$ 15 mGy and DLP 600 mGycm in abdominal CT), (STUK, 2013), but the use of DRL did not identify suboptimal protocols for larger patients, since the DRLs are only intended for patients with a weight between 60 kg and 90 kg. Larger patients need higher radiation doses than smaller patients to achieve predetermined noise levels in CT-images, but there is currently no measure of what degree of dose increase is acceptable for larger patients. With larger patients more noise can be moderated in images when the increase in radiation dose can be lower than predicted. Thus, there is a need for wider dose monitoring and for collecting all patient doses. With dose monitoring software, the doses can be reliably benchmarked in relation to other scanners, compared to DRLs or setting local DRLs, as the software collects and presents large data. The dose monitoring software aids in recognizing high doses that do not contribute to clinical purpose of medical imaging task or large size of patient, and action to improve the protocols can be undertaken. This might also indicate a need for setting DRLs as curves, as is the case for pediatric patients (STUK, 2015). DRL-curves could use with higher confidence, as dose monitoring software tools offer larger dose data together with data on patient size or patient dimensions (especially width). Previously data on patient size has not been collected systematically and patient width has not been measured. Dose monitoring software can determine patient width from localizer radiographs and this data could be used in conjunction with DRL-curves. For now, there is a limited number of indication-based DRLs, and a wider selection of DRLs may be needed to identify non-optimized protocols by dose monitoring software (STUK, 2013; STUK, 2015). In study III, the 75th percentiles of the radiation burden from CT studies needed to examine trauma to the cervical spine with the Aquilion One scanner could be used as local DRLs, while there seems

to be a need for local DRLs to be applied to the Definition Flash scanner as the $CTDI_{vol}$ values were clearly not optimal. Local DRLs can be set according to patient age, which is reasonable when studying the head or cervical spine, but age is not suitable parameter when establishing DRLs for thorax or abdominal CTs since the body size of patients with identical age may vary significantly. There may also be a need for other tools than DRLs to improve optimization.

Optimization is needed for patients of different size, as suggested in study V, since the protocol function may not be optimal for large patients. The TCM did not modulate when large patients were examined with the LightSpeed 16, and the increase in effective doses was higher for the LightSpeed 16 than the Plus 4 for patients with a wide waist circumference. This observation that larger patients are studied with non-optimal protocols is in agreement with recent statements of medical societies including the EFOMP and ESR, who call for BMI-specific protocol optimization (EANM et al., 2017). For assessment of the impact of BMI on $CTDI_{vol}$ and DLP, weight and height data should be recorded together with CT-study related data. In study V, height and weight were only recorded at the time of the first follow-up CT scan. Thus, data was obsolete at the time of subsequent CT studies, because patient size changes during follow-up. This made the waist circumference measured in connection each CT study a more reliable indicator of patient size. In the future, the recording of weight and height may become more common when dose monitoring software tools become more widely used and BMI-specific protocols are used for optimization.

Because AYA patients have a long life expectancy, the risk associated with imaging should be kept as low as reasonably possible. In order to keep the radiation dose at a minimum, the individual examinations need to be optimized and optimization should be done for special indications, as well. In study II, protocol parameters for acute appendicitis were determined with a specially planned phantom. After assessment of the dose, FOM and image quality, a new protocol with 100 kVp and standard IR was proposed for CT-imaging of patients with a suspicion of appendicitis. Higher contrast, acceptable noise and a lower dose was produced by 100 kVp and the radiologists evaluated image quality by the reference protocol and the new protocol as being similar. The new low-dose protocol fulfils the ALARA principle and implies that the original abdominal protocol may not have been optimized. The results agree with the ones of Kidoh et al, who also showed that standard iteration is more effective for dose reduction than strong IR while image quality is acceptable (Kidoh et al., 2013). The new protocol will be tested clinically to confirm the feasibility of a lower dose and the capability of the protocol to distinguish complicated from non-complicated acute appendicitis. The new protocol may also be considered for other indications of abdominal CT studies, *e.g.*, testicular cancer.

More attention should also be paid on the selection of parameters for localizer radiographs. An important finding of these studies is that localizer radiographs contribute significantly to the effective dose. The dose from a single localizer radiograph is small but the contribution may become substantial when the effective dose from a study is low, as is the case for

pediatric imaging. In study I, the localizer paragraphs contributed 13 % 24 % to the total effective dose of the study. This observation is in line the one of Schmidt et al, who reported a 5 % contribution to the dose in standard scans and a 20 % contribution to low-dose examinations of adult patients (Schmidt et al., 2013). The contribution to the effective dose from localizer radiographs should be as low as possible, since localizer radiographs are not used for diagnosis.

7 CONCLUSIONS

The conclusions of this thesis are

- I. There was a wide variation of radiation doses to the neonate chest CT studies, which was due to the differences between the CT scanners. The CT localizer radiographs can contribute significantly to the dose of newborn patients and the parameters of localizer radiographs should be reviewed in the same way as the parameters of the scanning procedure.
- II. A tube voltage of 100 kVp produced higher contrast to noise ratios than other voltages and generated a lower radiation dose without degrading the image quality. The phantom study resulted a 23 % lower dose with 100 kVp, standard iterative reconstruction and a noise input value of 14.5, but the protocols need to be tested in the clinical setting appendicitis imaging.
- III. Local diagnostic reference levels for CT-studies of the cervical spine following trauma are proposed for four different age groups. The study shows that more widespread dose monitoring is needed in situations where non-optimized CT doses can be detected directly and the effects of protocol changes can be studied more reliable from large data.
- IV. The study revealed that patients with testicular cancer are subject to relatively high cumulative doses – 50 mSv or more for 68 % of these patients. Although this study population constitutes a homogeneous cohort and is treated for the same indication, there was a 9-fold difference in organ doses and up to a 6-fold difference in effective doses. The high cumulative doses call for updated clinical practices regarding the frequency of CT imaging for follow-up purposes to keep patient exposure as low as reasonably achievable, since the benefit of repeated CT-imaging must be viewed against how well imaging detects cancer recurrence and what the treatment options in that situation entail.
- V. The CT scanner and use of IV contrast affect significantly the radiation dose. The newer device equipped with tube current modulation (TCM) produced higher doses for patients with a high waist circumference. This finding calls for patient size specific protocol optimization and assessment of the success of optimization.

ACKNOWLEDGEMENTS

This study was carried out at the Medical Imaging Centre of Southwest Finland and the Department of medical physics, Turku University Hospital, and the Department of Radiology, University of Turku during the years 2013-2017. It was financially supported by grants from Turku University Hospital (EVO grants), University of Turku and a grant from the Radiological Society of Finland.

First and above all, I own my deepest gratitude for my supervisors Professor Jarmo Kulmala, Professor Eeva Salminen and Adjunct professor Timo Kiljunen for guidance and support throughout the years. You taught me the scientific thinking and without your guidance this work could not have been done. I am grateful for your patience and helpful comments and corrections to the manuscripts and thesis.

I wish to thank the official reviewers, Professor Hans Ringertz and Adjunct professor Paula Toroi, for your constructive comments. Your valuable feedback resulted in distinct improvements in this thesis.

I would like to thank my supervisory board members, Professor Pekka Hänninen, Erkki Svedström, MD and medical physicist Jani Saunavaara. Your enthusiasm is contagious and you always have new ideas on what to study next or how to improve medical imaging.

I owe my sincere gratitude to OPTICAP-group Paulina Salminen, MD, Juha Grönroos, MD, Irina Rinta-Kiikka, MD, Suvi Sippola, MD, and Johanna Virtanen, MD, for your contribution to this work. I have been privileged to work with you and I appreciate your valuable comments. I hope that our collaboration will continue in the future. I sincerely thank my co-authors Principal Advisor Hannu Järvinen and medical physicist Minna Huuskonen. I am grateful for the statisticians Saija Hurme, Tuukka Pölönen and Simo Teperi, who performed the statistical analyses and explained with great patience the terms and methods multiple times.

I wish to thank Robet Paul for the linguistic revisions of the thesis and making it look like English language.

I would like to express my gratitude to the Chief physicist Mika Teräs for the possibility to have study leave to complete my thesis and finally reach the last milestone in the qualification as a medical physicist. I wish to thank all of the personnel at the Medical Imaging Center of Southwest Finland, especially Roberto Blanco Sequieros, the Chairman of the Medical Imaging Center of Southwest Finland for providing the research facilities. My warm thanks go to all of the radiologist and radiographers with whom I have been working with. I would also like to express my deepest gratitude to all my physicist colleagues, especially Heli Määttänen and Jukka Järvinen, who have given me guidance during these years and divided their knowledge. I have been privileged to work with you.

My friends, 'the Norro clan' and the ladies of Turku Accordeon orchestra are thanked for great company and joyful moments spent together.

I want to thank my siblings Heli and Veli-Matti and their families. You have provided me valuable breaks during the studies and the liveliness of the little nieces and nephews has brought happiness to my life. I'm lucky to have such great persons in my life. I want also show my deepest gratitude to my dear parents, Hilikka and Matti, who have always supported me during all these years.

And to you Toni, my dear husband and the love of my life: "Are we an effective team?" Yes, we are ;)

Turku, August 2017

Hannele Niiniviita

REFERENCES

- AAPM - American association of physicists in medicine (2008). The measurement, reporting, and management of radiation dose in CT. AAPM Report No. 96, AAPM.
- AAPM - American association of physicists in medicine (2011). Size specific dose estimate (SSDE) in pediatric and adult body CT examinations. AAPM Report No. 204, AAPM.
- Alessio, A. M. and Phillips, G. S. (2010). A pediatric CT dose and risk estimator. *Pediatric radiology*, 40(11):1816-1821.
- American Cancer Society (2016). Cancer facts & Figures 2016. American Cancer Society, Atlanta, USA.
- Bahadori, A., Miglioretti, D., Kruger, R., Flynn, M., Weinmann, S., Smith-Bindman, R., and Lee, C. (2015). Calculation of organ doses for a large number of patients undergoing computed tomography examinations. *AJR. American journal of roentgenology*, 205(4):827-833.
- Beckett, K. R., Moriarty, A. K., and Langer, J. M. (2015). Safe use of contrast media: What the radiologist needs to know. *RadioGraphics*, 35(6):1738-1750.
- BEIR - Committee to Assess Health Risks from Exposure to Low Levels of Ionizing Radiation (2006). Health Risks from Exposure to Low Levels of Ionizing Radiation: BEIR VII Phase 2. National Research Council of the National Academies Press, Washington DC, USA.
- Beister, M., Kolditz, D., and Kalender, W. A. (2012). Iterative reconstruction methods in x-ray CT. *Physica medica*, 28(2):94-108.
- Blomstrand, M., Holmberg, E., Aberg, M. A., Lundell, M., Bjork-Eriksson, T., Karlsson, P., and Blomgren, K. (2014). No clinically relevant effect on cognitive outcomes after low-dose radiation to the infant brain: a population-based cohort study in Sweden. *Acta Oncologica*, 53(9):1143-1150.
- Boetticher, H., Lachmund, J., Looe, H. K., Hoffmann, W., and Poppe, B. (2008). 2007 recommendations of the ICRP change basis for estimation of the effective dose: what is the impact on radiation dose assessment of patient and personnel? *RoFo: Fortschritte auf dem Gebiete der Rontgenstrahlen und der Nuklearmedizin*, 180(5):391-395.
- Bonassi, S., Norppa, H., Ceppi, M., Stromberg, U., Vermeulen, R., Znaor, A., Cebulka-Wasilewska, A., Fabianova, E., Fucic, A., Gundy, S., Hansteen, I. L., Knudsen, L. E., Lazutka, J., Rossner, P., Sram, R. J., and Boffetta, P. (2008). Chromosomal aberration frequency in lymphocytes predicts the risk of cancer: results from a pooled cohort study of 22 358 subjects in 11 countries. *Carcinogenesis*, 29(6):1178-1183.
- Bondt, T. D., Mulken, T., Zanca, F., Pyfferoen, L., Caselman, J. W., and Parizel, P. M. (2016). Benchmarking pediatric cranial CT protocols using a dose tracking software system: a multicenter study. *European radiology*, doi:10.1007/s00330-016-4385-4.
- Boone, J. M. (2007). The trouble with CTD100. *Medical physics*, 34(4):1364-1371.
- Boos, J., Meineke, A., Bethge, O. T., Antoch, G., and Kropil, P. (2016). Dose monitoring in radiology departments: Status quo and future perspectives. *RoFo: Fortschritte auf dem Gebiete der Rontgenstrahlen und der Nuklearmedizin JID - 7507497*, 188(5):443.
- Brenner, D. J. (2008). Effective dose: a flawed concept that could and should be replaced. *The British journal of radiology*, 81(967):521-523.
- Brenner, D. J., Doll, R., Goodhead, D. T., Hall, E. J., Land, C. E., Little, J. B., Lubin, J. H., Preston, D. L., Preston, R. J., Puskin, J. S., Ron, E., Sachs, R. K., Samet, J. M., Setlow, R. B., and Zaider, M. (2003). Cancer risks attributable to low doses of ionizing radiation: assessing what we really know. *Proceedings of the National Academy of Sciences of the United States of America*, 100(24):13761-13766.
- Brenner, D. J. and Hall, E. J. (2007). Computed tomography increasing source of radiation exposure. *The New England journal of medicine*, 357(22):2277-2284.
- Buchler, T., Kubankova, P., Boublikova, L., Donatova, Z., Foldyna, M., Kanakova, J., Kordikova, D., Kupec, M., Nepomucka, J., Vorsilkova, E., and Abrahamova, J. (2011). Detection of second malignancies during long-term follow-up of testicular cancer survivors. *Cancer*, 117(18):4212-4218.
- Buls, N., Bosmans, H., Mommaert, C., Malchair, F., Clapuyt, P., and Everarts, P. (2010). Ct paediatric doses in Belgium: a multi-centre - study results from a dosimetry audit in 2007-2009. *Belgian Federal Agency of Nuclear Control (FANC)*.

- Bushberg, J. T., Seibert, J. A., Leidholdt, E. M., and Boone, J. M. (2012). *The essential physics of medical imaging* 3rd ed. Wolters Kluwer, Lippincott Williams & Wilkins, Philadelphia, USA.
- Cakmak, E. D., Tuncel, N., and Sindir, B. (2015). Assessment of organ dose by direct and indirect measurements for a wide bore x-ray computed tomography unit that used in radiotherapy. *IJMP. International Journal of Medical Physics*, 4:132-142.
- Calandrino, R., Ardu, V., Corletto, D., del Vecchio, A., Origgi, D., Signorotto, P., Spinelli, A., Tosi, G., Bolognesi, A., Cariati, M., Kluzer, A., and Muscarella, S. (2013). Evaluation of second cancer induction risk by CT follow-up in oncological long-surviving patients. *Health physics*, 104(1):1-8.
- Carinou, E., Boziari, A., Askounis, P., Mikulis, A., and Kamenopoulou, V. (2008). Energy dependence of TD 100 and MCP-N detectors. *Radiation Measurements*, 43(2-6):599-602.
- de Gonzalez, A. B. and Kleinerman, R. A. (2015). CT scanning: Is the contrast material enhancing the radiation dose and cancer risk as well as the image? *Radiology*, 275(3):627-629.
- Deak, P. D., Smal, Y., and Kalender, W. A. (2010). Multisection CT protocols: sex- and age-specific conversion factors used to determine effective dose from dose-length product. *Radiology*, 257(1):158-166.
- Deinzer, C. K., Danova, D., Kleb, B., Klose, K. J., and Heverhagen, J. T. (2014). Influence of different iodinated contrast media on the induction of DNA double-strand breaks after in vitro x-ray irradiation. *Contrast media & molecular imaging*, 9(4):259-267.
- Ding, A., Gao, Y., Liu, H., Caraccappa, P. F., Long, D. J., Bolch, W. E., Liu, B., and Xu, X. G. (2015). Virtual-dose: a software for reporting organ doses from CT for adult and pediatric patients. *Physics in Medicine and Biology*, 60(14):5601-5625.
- Duggan, L., Hood, C., Warren-Forward, H., Haque, M., and Kron, T. (2004). Variations in dose response with x-ray energy of LiF:Mg,Cu,P thermoluminescence dosimeters: implications for clinical dosimetry. *Physics in Medicine and Biology*, 49(17):3831-3845.
- EANM - European Association of Nuclear Medicine, EFOMP – European Federation of Organizations for Medical Physics, EFRS – European Federation of Radiographer Societies, ESR - European Society of Radiology, and ESTRO - European Society for Radiotherapy and Oncology (2017). *Common strategic research agenda for radiation protection in medicine. Insights into imaging*, doi:10.1007/s13244-016-0538-x.
- EC - European Commission (1999). *Radiation protection no 109. Guidance on diagnostic reference levels (DRLs) for medical exposures*. European Commission, Luxembourg.
- EC - European Commission (2012). *Radiation protection no 162. Medical radiation exposure of the european population*. European Commission, Luxembourg.
- EC - European Commission (2015). *Radiation protection no 180. Criteria for acceptability of medical radiological equipment used in diagnostic radiology, nuclear medicine and radiotherapy, part 1/2*. European Commission, Luxembourg.
- EU - The council of the European Union (2013). *Council directive 2013/59/euratom*. 2016:10/3.
- Fazel, R., Krumholz, H. M., Wang, Y., Ross, J. S., Chen, J., Ting, H. H., Shah, N. D., Nasir, K., Einstein, A. J., and Nallamothu, B. K. (2009). Exposure to low-dose ionizing radiation from medical imaging procedures. *N Engl J Med*, 361(9):849-857.
- Fiechter, M., Stehli, J., Fuchs, T. A., Dougoud, S., Gaemperli, O., and Kaufmann, P. A. (2013). Impact of cardiac magnetic resonance imaging on human lymphocyte DNA integrity. *European heart journal*, 34(30):2340-2345.
- Fält, T., Söderberg, M., Hörberg, L., Carlgren, I., and Leander, P. (2013). Seesaw balancing radiation dose and i.v. contrast dose: evaluation of a new abdominal CT protocol for reducing age-specific risk. *AJR. American journal of roentgenology*, 200(2):383-388.
- Geleijns, J., Artells, M. S., de Bruin, P. W., Matter, R., Muramatsu, Y., and McNitt-Gray, M. F. (2009). Computed tomography dose assessment for a 160 mm wide, 320 detector row, cone beam CT scanner. *Physics in Medicine and Biology*, 54(10):3141-3159.
- Geyer, L. L., Schoepf, U. J., Meinel, F. G., Nance, J. W., Bastarrica, G., Leipsic, J. A., Paul, N. S., Rengo, M., Laghi, A., and Cecco, C.
- N. D. (2015). State of the art: Iterative CT reconstruction techniques. *Radiology*, 276(2):339-357.
- Goo, H. W. (2012). CT radiation dose optimization and estimation: an update for radiologists. *Korean journal of radiology*, 13(1):1-11.
- Griffey, R. T. and Sodickson, A. (2009). Cumulative radiation exposure and cancer risk estimates in emergency department patients undergoing repeat or multiple CT. *AJR. American journal of roentgenology*, 192(4):887-892.
- Groves, A. M., Owen, K. E., Courtney, H. M., Yates, S. J., Goldstone, E., and A.K., D. B. (2004). 16-detector multislice CT: dosimetry estimation by TLD measurement compared with Monte Carlo simulation. *The British Journal of Radiology*, 77:662-665.

- Hall, P., Adami, H. O., Trichopoulos, D., Pedersen, N. L., Lagiou, P., Ekblom, A., Ingvar, M., Lundell, M., and Granath, F. (2004). Effect of low doses of ionising radiation in infancy on cognitive function in adulthood: Swedish population based cohort study. *BMJ (Clinical research ed.)*, 328(7430):19.
- Higashigaito, K., Becker, A. S., Sprengel, K., Simmen, H. P., Wanner, G., and Alkadhi, H. (2016). Automatic radiation dose monitoring for CT of trauma patients with different protocols: feasibility and accuracy. *Clinical radiology*, 71(9):905-911.
- Hough, M., Johnson, P., Rajon, D., Jokisch, D., Lee, C., and Bolch, W. (2011). An image-based skeletal dosimetry model for the ICRP reference adult male - internal electron sources. *Physics in Medicine and Biology*, 56(8):2309-2346.
- Hranitzky, C., Stadtmann, H., and Olko, P. (2006). Determination of LiF:Mg,Ti and LiF:Mg,Cu,P TL efficiency for x-rays and their application to monte carlo simulations of dosimeter response. *Radiation Protection Dosimetry*, 119(1-4):483-486.
- Huda, W., Magill, D., and He, W. (2011). CT effective dose per dose length product using ICRP 103 weighting factors. *Medical physics*, 38(3):1261-1265.
- Huda, W., Ogden, K. M., and Khorasani, M. R. (2008). Converting doselength product to effective dose at CT. *Radiology*, 248(3):995-1003.
- Huda, W., Scalzetti, E. M., and Levin, G. (2000). Technique factors and image quality as functions of patient weight at abdominal CT. *Radiology*, 217(2):430-435.
- IAEA - International Atomic Energy Agency (2007). Dosimetry in diagnostic radiology: an international code of practice. Technical Reports Series no. 457, IAEA.
- ICRP - International Commission on Radiological Protection (1977). Recommendations of the international commission on radiological protection. ICRP publication 26. *Annals of the ICRP*, 1(3).
- ICRP - International Commission on Radiological Protection (1979). Report of the task group on reference man. ICRP publication 23. *Annals of the ICRP*, 3(1-4).
- ICRP - International Commission on Radiological Protection (1991). Recommendations of the international commission on radiological protection. ICRP publication 60. *Annals of the ICRP*, 21(1-3).
- ICRP - International Commission on Radiological Protection (1996). Radiological protection and safety in medicine. ICRP publication 73. *Annals of the ICRP*, 73, 26(2):1-31.
- ICRP - International Commission on Radiological Protection (2007). The 2007 recommendations of the international commission on radiological protection. ICRP publication 103. *Annals of the ICRP*, 37(2-4):1-332.
- ICRP - International Commission on Radiological Protection (2009). Adult reference computational phantoms. ICRP publication 110. *Annals of the ICRP*, 39(2).
- ICRP - International Commission on Radiological Protection (2013). Radiological protection in paediatric diagnostic and interventional radiology. ICRP publication 121. *Annals of the ICRP*, 42(2):1-63.
- ICRU - International Commission on Radiation Units and Measurements (1992). ICRU report no. 48, phantoms and computational models in therapy, diagnosis and protection. *Journal of the International Commission on Radiation Units and Measurements*, 25(1).
- ICRU - International Commission on Radiation Units and Measurements (2005a). ICRU report no. 74, patient dosimetry for x-rays used in medical imaging. *Journal of the International Commission on Radiation Units and Measurements*, 5(2).
- ICRU - International Commission on Radiation Units and Measurements (2005b). Methods for determining organ and tissue doses. *Journal of the International Commission on Radiation Units and Measurements*, 5(2):55-62.
- ICRU - International Commission on Radiation Units and Measurements (2012). ICRU report no. 87, radiation dose and image-quality assessment in computed tomography. *Journal of the International Commission on Radiation Units and Measurements*, 12(1):1-149.
- IEC - International Electrotechnical Commission (2009). IEC 60601-2-44 ed.3: Medical electrical equipment - part 2-44: Particular requirements for the basic safety and essential performance of x-ray equipment for computed tomography.
- Impactscan. Website: www.impactscan.org/ctdosimetry.htm, referred at 18/4/2017.
- Jackson, D., Atkin, K., Bettenay, F., Clark, J., Ditchfield, M. R., Grimm, J. E., Linke, R., Long, G., Onikul, E., Pereira, J., Phillips, M., Wilson,
- F., Paul, E., and Goergen, S. K. (2015). Paediatric CT dose: a multicenter audit of subspecialty practice in Australia and New Zealand. *European radiology*, 25(11):3109-3122.
- Jaffer, H. and Murphy, K. J. (2017). Magnetic resonance imaging-induced DNA damage. *Canadian Association of Radiologists journal*, 68(1):2-3.

- Jansen, J. T. and Shrimpton, P. C. (2016). Development of Monte Carlo simulations to provide scanner-specific organ dose coefficients for contemporary CT. *Physics in Medicine and Biology*, 61(14):5356-5377.
- Jones, D. G. and Shrimpton, P. C. (1993). Normalised organ doses for X-ray computed tomography calculated using Monte Carlo techniques. *Radiat Prot Dosimetry*, 49:241.
- Kaasalainen, T., Palmu, K., Lampinen, A., and Korteniemi, M. (2013). Effect of vertical positioning on organ dose, image noise and contrast in pediatric chest CT phantom study. *Pediatric radiology*, 43(6):673-684.
- Kalender, W. A. (2011). *Computed tomography: Fundamentals, system technology, image quality, applications*, 3rd edition. Publicis Publishing, Erlangen, Germany.
- Kalender, W. A., Buchenau, S., Deak, P., Kellermeier, M., Langner, O., van Straten, M., Vollmar, S., and Wilham, S. (2008). Technical approaches to the optimisation of CT. *Physica medica*, 24(2):71-79.
- Kalra, M. K., Maher, M. M., Toth, T. L., Hamberg, L. M., Blake, M. A., Shepard, J. A., and Saini, S. (2004). Strategies for CT radiation dose optimization. *Radiology*, 230(3):619-628.
- Karmazyn, B., Liang, Y., Klahr, P., and Jennings, S. G. (2013). Effect of tube voltage on CT noise levels in different phantom sizes. *AJR. American journal of roentgenology*, 200(5):1001-1005.
- Khursheed, A., Hillier, M. C., Shrimpton, P. C., and Wall, B. F. (2002). Influence of patient age on normalized effective doses calculated for CT examinations. *The British journal of radiology*, 75(898):819-830.
- Kidoh, M., Nakaura, T., Nakamura, S., Oda, S., Utsunomiya, D., Sakai, Y., Harada, K., and Yamashita, Y. (2013). Low-dose abdominal CT: comparison of low tube voltage with moderate-level iterative reconstruction and standard tube voltage, low tube current with high-level iterative reconstruction. *Clinical radiology*, 68(10):1008-1015.
- Kim, J. S., Kwon, S. M., Kim, J. M., and Yoon, S. W. (2017). New organ-based tube current modulation method to reduce the radiation dose during computed tomography of the head: evaluation of image quality and radiation dose to the eyes in the phantom study. *La Radiologia medica*. doi: 10.1007/s11547-017-0755-5
- Kim, M., Lee, J. M., Yoon, J. H., Son, H., Choi, J. W., Han, J. K., and Choi, B. I. (2014). Adaptive iterative dose reduction algorithm in CT: effect on image quality compared with filtered back projection in body phantoms of different sizes. *Korean journal of radiology*, 15(2):195-204.
- Kim, Y. Y., Shin, H. J., Kim, M. J., and Lee, M. J. (2016). Comparison of effective radiation doses from x-ray, CT, and PET/CT in pediatric patients with neuroblastoma using a dose monitoring program. *Diagnostic and interventional radiology (Ankara, Turkey)*, 22(4):390-394.
- Kron, T. (1999). Applications of thermoluminescence dosimetry in medicine. *Radiation Protection Dosimetry*, 85(1-4):333-340.
- Lee, C. H., Goo, J. M., Ye, H. J., Ye, S. J., Park, C. M., Chun, E. J., and Im, J. G. (2008). Radiation dose modulation techniques in the multidetector CT era: from basics to practice. *Radiographics*, 28(5):1451.
- Lusic, H. and Grinstaff, M. W. (2012). X-ray computed tomography contrast agents. *Chemical reviews*, 113(3):10.1021/cr200358s.
- Marin, D., Nelson, R. C., Schindera, S. T., Richard, S., Youngblood, R. S., Yoshizumi, T. T., and Samei, E. (2010). Low-tube-voltage, hightube-current multidetector abdominal CT: improved image quality and decreased radiation dose with adaptive statistical iterative reconstruction algorithm - initial clinical experience. *Radiology*, 254(1):145-153.
- Martin, C. (2007a). The importance of radiation quality for optimization in radiology. *Biomedical imaging and intervention journal*, 3(2):e38.
- Martin, C. J. (2007b). Effective dose: how should it be applied to medical exposures? *The British journal of radiology*, 80(956):639-647.
- Mathews, J. D., Forsythe, A. V., Brady, Z., Butler, M. W., Goergen, S. K., Byrnes, G. B., Giles, G. G., Wallace, A. B., Anderson, P. R.,
- Guiver, T. A., McGale, P., Cain, T. M., Dowty, J. G., Bickelstaffe, A. C., and Darby, S. C. (2013). Cancer risk in 680,000 people exposed to computed tomography scans in childhood or adolescence: data linkage study of 11 million australians. *BMJ (Clinical research ed.)*, 346:f2360.
- Matsubara, K., Koshida, K., Ichikawa, K., Suzuki, M., Takata, T., Yamamoto, T., and Matsui, O. (2009). Misoperation of CT automatic tube current modulation systems with inappropriate patient centering: phantom studies. *AJR. American journal of roentgenology*, 192(4):862-865.
- Mayo-Smith, W., Hara, A. K., Mahesh, M., Sahani, D. V., and Pavlicek, W. (2014). How i do it: Managing radiation dose in CT. *Radiology*, 273(3):657-672.
- McCollough, C. H., Leng, S., Yu, L., Cody, D. D., Boone, J. M., and McNitt-Gray, M. F. (2011). CT dose index and patient dose: they are not the same thing. *Radiology*, 259(2):311-316.

- McCullough, C. H., Primak, A. N., Braun, N., Koffler, J., Yu, L., and Christner, J. (2009). Strategies for reducing radiation dose in CT. *Radiologic clinics of North America*, 47(1):27-40.
- Mettler, F. A. J., Thomadsen, B. R., Bhargavan, M., Gillely, D. B., Gray, J. E., Lipoti, J. A., McCrohan, J., Yoshizumi, T. T., and Mahesh, M. (2008). Medical radiation exposure in the U.S. in 2006: preliminary results. *Health physics*, 95(5):502-507.
- Metzner, J., Posner, K. L., and Domino, K. B. (2009). The risk and safety of anesthesia at remote locations: the US closed claims analysis. *Current opinion in anaesthesiology*, 22(4):502-508.
- Miglioretti, D. L., Johnson, E., Williams, A., Greenlee, R. T., Weinmann, S., Solberg, L. I., Feigelson, H. S., Roblin, D., Flynn, M. J., Vanneman, N., and Smith-Bindman, R. (2013). The use of computed tomography in pediatrics and the associated radiation exposure and estimated cancer risk. *JAMA pediatrics*, 167(8):700-707.
- Miller, D. L., Vano, E., and Rehani, M. M. (2015). Reducing radiation, revising reference levels. *Journal of the American College of Radiology: JACR*, 12(3):214-216.
- Ministry of Social Affairs and Health (2016). Medical research act no. 488/1999. Original text in Finnish.
- Moore, B. M., Brady, S. L., Mirro, A. E., and Kaufman, R. A. (2014). Size-specific dose estimate (SSDE) provides a simple method to calculate organ dose for pediatric CT examinations. *Medical physics*, 41(7):071917.
- Muikko, M., Bly, R., Kurtio, P., Lahtinen, J., Lehtinen, M., Siiskonen, T., Turtiainen, T., Valmari, T., and Vesterbacka, K. (2014). Suomalaisten keskimääräinen efektiivinen annos, annoskaku 2012. Original text in Finnish. STUK-A259.
- NCRP - National Council on Radiation Protection and Measurements (1993). Limitation of exposure to ionizing radiation. NCRP Report No. 116. Bethesda, MD, USA.
- Nickoloff, E. L., Dutta, A. K., and Lu, Z. F. (2003). Influence of phantom diameter, kvp and scan mode upon computed tomography dose index. *Medical physics*, 30(3):395-402.
- Norris, H., Zhang, Y., Bond, J., Sturgeon, G. M., Minhas, A., Tward, D. J., Ratnanather, J. T., Miller, M. I., Frush, D., Samei, E., and Segars, W. P. (2014). A set of 4D pediatric XCAT reference phantoms for multimodality research. *Medical physics*, 41(3):033701.
- O'Connell, O. J., McWilliams, S., McGarrigle, A., O'Connor, O. J., Shanahan, F., Mullane, D., Eustace, J., Maher, M. M., and Plant, B. J. (2012). Radiologic imaging in cystic fibrosis: cumulative effective dose and changing trends over 2 decades. *Chest*, 141(6):1575-1583.
- Padole, A., Khawaja, R. D. A., Kalra, M. K., and Singh, S. (2015). CT radiation dose and iterative reconstruction techniques. *AJR. American journal of roentgenology*, 204(4):W384-92.
- Pearce, M. S., Salotti, J. A., Little, M. P., McHugh, K., Lee, C., Kim, K. P., Howe, N. L., Ronckers, C. M., Rajaraman, P., Craft, A. W. S., Parker, L., and de Gonzalez, A. B. (2012). Radiation exposure from CT scans in childhood and subsequent risk of leukaemia and brain tumours: a retrospective cohort study. *Lancet*, 380(9840):499-505.
- Piechowiak, E. I., Peter, J. F., Kleb, B., Klose, K. J., and Heverhagen, J. T. (2015). Intravenous iodinated contrast agents amplify DNA radiation damage at CT. *Radiology*, 275(3):692-697.
- Pradhan, A. S., Kim, J. L., and Lee, J. I. (2012). On the use of "effective dose" in medical exposures. *Journal of medical physics*, 37(2):63-65.
- Preston, D. L., Ron, E., Tokuoka, S., Funamoto, S., Nishi, N., Soda, M., Mabuchi, K., and Kodama, K. (2007). Solid cancer incidence in atomic bomb survivors: 1958-1998. *Radiation research*, 168(1):1-64.
- Rohner, D. J., Bennett, S., Samaratunga, C., Jewell, E. S., Smith, J. P., Gaskill-Shiple, M., and Lisco, S. J. (2013). Cumulative total effective whole-body radiation dose in critically ill patients. *Chest*, 144(5):1481-1486.
- Sagara, Y., Hara, A. K., Pavlicek, W., Silva, A. C., Paden, R. G., and Wu, Q. (2010). Abdominal CT: comparison of low-dose CT with adaptive statistical iterative reconstruction and routine-dose CT with filtered back projection in 53 patients. *AJR. American journal of roentgenology*, 195(3):713-719.
- Salminen, E., Niiniviita, H., Jarvinen, H., and Heinavaara, S. (2017). Cancer death risk related to radiation exposure from computed tomography scanning among testicular cancer patients. *Anticancer Research*, 37(2):831-834.
- Salminen, P., Paajanen, H., Rautio, T., Nordström, P., Aarnio, M., Rantanen, T., Tuominen, R., Hurme, S., Virtanen, J., Mecklin, J., Sand, J., Jartti, A., Rinta-Kiikka, I., and Grönroos, J. M. (2015). Antibiotic therapy vs appendectomy for treatment of uncomplicated acute appendicitis: the APPAC randomized clinical trial. *JAMA*, 313(23):2340-2348.

- Samei, E., 3rd, J. T. D., Lo, J. Y., and Tornai, M. P. (2005). A framework for optimising the radiographic technique in digital x-ray imaging. *Radiation Protection Dosimetry*, 114(1-3):220-229.
- Schmidt, B., Salybaeva, N., Kolditz, D., and Kalender, W. A. (2013). Assessment of patient dose from CT localizer radiographs. *Medical physics*, 40(8):084301.
- Segars, W. P., Bond, J., Frush, J., Hon, S., Eckersley, C., Williams, C. H., Feng, J., Tward, D. J., Ratnanather, J. T., Miller, M. I., Frush, D., and Samei, E. (2013). Population of anatomically variable 4D XCAT adult phantoms for imaging research and optimization. *Medical physics*, 40(4):043701.
- Segars, W. P., Mahesh, M., Beck, T. J., Frey, E. C., and Tsui, B. M. (2008). Realistic CT simulation using the 4D XCAT phantom. *Medical physics*, 35(8):3800-3808.
- Sender, L. and Zabokrtsky, K. B. (2015). Adolescent and young adult patients with cancer: a milieu of unique features. *Nature reviews. Clinical oncology*, 12(8):465-480.
- Shrimpton, P. C. (2004). Assessment of patient dose in CT. nrbpe/1/2004. Technical report, National Radiological Protection Board (NRPB).
- Shrimpton, P. C., Hillier, M. C., Lewis, M. A., and Dunn, M. (2005). National survey of doses from CT in the UK: 2003 review. Technical Report NRPB-W67, National Radiological Protection Board.
- Shrimpton, P. C., Hillier, M. C., Meeson, S., and Golding, S. J. (2014). Doses from computed tomography (CT) examinations in the UK - 2011 review. Technical Report PHE-CRCE-013, Centre for Radiation, Chemical and Environmental Hazards.
- Silva, M. V., Motamedinia, P., Badalato, G. M., Hruby, G., and McKiernan, J. M. (2012). Diagnostic radiation exposure risk in a contemporary cohort of male patients with germ cell tumor. *The Journal of urology*, 187(2):482-486.
- Soderberg, M. and Gunnarsson, M. (2010). Automatic exposure control in computed tomography - an evaluation of systems from different manufacturers. *Acta Radiologica*, 51(6):625-634.
- Stark, D. P. and Vassal, G. (2016). Tumors in Adolescents and Young Adults, Progress in tumor research; v. 43, page 117. Karger, Basel, Switzerland.
- Stiles, B. M., Mirza, F., Towe, C. W., Ho, V. P., Port, J. L., Lee, P. C., Paul, S., Yankelevitz, D. F., and Altorki, N. K. (2011). Cumulative radiation dose from medical imaging procedures in patients undergoing resection for lung cancer. *The Annals of Thoracic Surgery*, 92(4):1170-1179.
- STUK - Säteilyturvakeskus, Radiation and Nuclear Safety Authority (2013). Potilaan säteilyaltistuksen vertailutasot aikuisten tietokonetomografiatutkimuksissa, pää-tös 2/3020/2013. (Reference levels for the patient's radiation exposure for adult CT scans, Decision 2/3020/2013). Original text in Finnish.
- STUK - Säteilyturvakeskus, Radiation and Nuclear Safety Authority (2015). Potilaan säteilyaltistuksen vertailutasot lasten tietokonetomografiatutkimuksissa, päätös 9/3020/2015 (Reference levels for the patient's radiation exposure for paediatric CT scans, Decision 9/3020/2015). Original text in Finnish.
- Sullivan, C. J., Murphy, K. P., McLaughlin, P. D., Twomey, M., K.N.O'Regan, Power, D., Maher, M., and O'Connor, O. (2015). Radiation exposure from diagnostic imaging in young patients with testicular cancer. *European Radiology*. 25(4):1005-1013.
- Suutari, J. (2016). Radiologisten tutkimusten ja toimenpiteiden määrät vuonna 2015. Original text in Finnish. STUK-B207.
- Tarin, T. V., Sonn, G., and Shinghal, R. (2009). Estimating the risk of cancer associated with imaging related radiation during surveillance for stage I testicular cancer using computerized tomography. *The Journal of urology*, 181(2):627-633.
- Thomas, K. E. and Wang, B. (2008). Age-specific effective doses for pediatric MSCT examinations at a large children's hospital using DLP conversion coefficients: a simple estimation method. *Pediatric radiology*, 38(6):645-656.
- Thomas, P., Hayton, A., Beveridge, T., Marks, P., and Wallace, A. (2015). Evidence of dose saving in routine CT practice using iterative reconstruction derived from a national diagnostic reference level survey. *The British journal of radiology*, 88(1053):20150380.
- Tian, X., Li, X., Segars, W. P., Frush, D. P., and Samei, E. (2015). Prospective estimation of organ dose in CT under tube current modulation. *Medical physics*, 42(4):1575-1585.
- UNSCEAR - United Nations Scientific Committee on the Effects of Atomic Radiation (2010). UNSCEAR 2008 Report: Sources and effects of ionizing radiation, volume Vol I. United Nations, New York.
- Verdun, F. R., Gutierrez, D., Vader, J. P., Aroua, A., Alamo-Maestre, L. T., Bochud, F., and Gudinchet, F. (2008). CT radiation dose in children: a survey to establish age-based diagnostic reference levels in Switzerland. *European radiology*, 18(9):1980-1986.
- Verdun, F. R., Racine, D., Ott, J. G., Tapiovaara, M. J., Toroi, P., Bochud, F. O., Veldkamp, W. J., Schegerer, A., Bouwman, R. W., Giron, I. H., Marshall, N. W., and Edyvean, S. (2015). Image quality in CT: From physical measurements to model observers. *Physica medica*, 31(8):823-843.

- Wichmann, J. L., Hardie, A. D., Schoepf, U. J., Felmly, L. M., Perry, J. D., Varga-Szemes, A., Mangold, S., Caruso, D., Canstein, C., Vogl, T. J., and Cecco, C. N. D. (2017). Single- and dual-energy CT of the abdomen: comparison of radiation dose and image quality of 2nd and 3rd generation dual-source CT. *European radiology*, 27(2):642-650.
- Yoshizumi, T. T., Goodman, P. C., Frush, D. P., Nguyen, G., Toncheva, G., Sarder, M., and Barnes, L. (2007). Validation of metal oxide semiconductor field effect transistor technology for organ dose assessment during CT: comparison with thermoluminescent dosimetry. *AJR. American journal of roentgenology*, 188(5):1332-1336.
- Yu, L., Bruesewitz, M. R., Thomas, K. B., Fletcher, J. G., Koer, J. M., and McCollough, C. H. (2011). Optimal tube potential for radiation dose reduction in pediatric CT: principles, clinical implementations, and pitfalls. *Radiographics: a review publication of the Radiological Society of North America, Inc*, 31(3):835-848.

Annales Universitatis Turkuensis



Turun yliopisto
University of Turku

ISBN 978-951-29-6941-8 (PRINT)
ISBN 978-951-29-6942-5 (PDF)
ISSN 0355-9483 (PRINT) | ISSN 2343-3213 (PDF)